



5-2019

Morphometrics and Phylogeography of the Cave-Obligate Land Snail *Helicodiscus barri* (Gastropoda, Stylommatophora, Helicodiscidae)

Nicholas Scott Gladstone
University of Tennessee, nlgadsto@vols.utk.edu

Follow this and additional works at: https://trace.tennessee.edu/utk_gradthes

Recommended Citation

Gladstone, Nicholas Scott, "Morphometrics and Phylogeography of the Cave-Obligate Land Snail *Helicodiscus barri* (Gastropoda, Stylommatophora, Helicodiscidae). " Master's Thesis, University of Tennessee, 2019.
https://trace.tennessee.edu/utk_gradthes/5430

This Thesis is brought to you for free and open access by the Graduate School at TRACE: Tennessee Research and Creative Exchange. It has been accepted for inclusion in Masters Theses by an authorized administrator of TRACE: Tennessee Research and Creative Exchange. For more information, please contact trace@utk.edu.

To the Graduate Council:

I am submitting herewith a thesis written by Nicholas Scott Gladstone entitled "Morphometrics and Phylogeography of the Cave-Obligate Land Snail *Helicodiscus barri* (Gastropoda, Stylommatophora, Helicodiscidae)." I have examined the final electronic copy of this thesis for form and content and recommend that it be accepted in partial fulfillment of the requirements for the degree of Master of Science, with a major in Geology.

Michael McKinney, Major Professor

We have read this thesis and recommend its acceptance:

Brian O'Meara, Colin D. Sumrall, Matthew Niemiller

Accepted for the Council:

Dixie L. Thompson

Vice Provost and Dean of the Graduate School

(Original signatures are on file with official student records.)

**Morphometrics and Phylogeography of the Cave-Obligate
Land Snail *Helicodiscus barri* (Gastropoda,
Stylommatophora, Helicodiscidae)**

A Thesis Presented for the
Master of Science
Degree
The University of Tennessee, Knoxville

Nicholas Scott Gladstone

May 2019

Copyright © 2019 by Nicholas S. Gladstone.

All rights reserved.

ACKNOWLEDGEMENTS

I would like to acknowledge several people for their contributions to my work throughout my Master's program. First, to Dr. McKinney, thanks for the seemingly endless amount of support you have given me in the six some odd years you have known me. I came into your office bright-eyed and clueless as an undergrad, and you decided to invest in me. To Dr. O'Meara, your guiding hand during both my undergrad and graduate programs has been invaluable, and I appreciate the time you've invested in me. To Dr. Niemiller, I emailed you a small rant about being interested in cave salamanders when I was 19, and you turned that into what now seems like a lifelong passion for working with subterranean organisms. Your patience, guidance, and friendship have meant the world to me. An additional thank you goes to the undergrads within the Niemiller Lab for their assistance with DNA extractions and PCR. To Dr. Carter, you have given me all the tools and knowhow I could have ever asked for to be successful as a scientist. I must have come to bother you hundreds of times in your office, and you stuck with me in hard times for the both of us. You're the reason why I was ready for graduate school, and above all you taught me to ask the right questions. To Evelyn Pieper, thank you for all your love and support throughout my time in graduate school. I couldn't have gotten through the long nights and frustrating field days without you by my side. Finally, I acknowledge the University of Tennessee, National Speleological Society, and the Conchologists' of America Organization for their generous funding that facilitated this research.

ABSTRACT

Molecular studies have recently led to the detection of many cryptic species complexes within morphologically ambiguous species formerly undescribed by the scientific community.

Organisms such as land snails are at a particularly high risk of species misidentification and misinterpretation, in that gastropod systematics are based almost entirely on external shell morphology. Subterranean ecosystems are associated with especially high degrees of cryptic speciation, largely owing to the abiotic similarities of these systems. In this study, I attempt to diagnose the potential cryptic diversity in the troglobitic land snail *Helicodiscus barri*. Land snails are generally associated with having low vagility, and as such this species' broad, mosaic distribution indicates the misdiagnosis of this organism as a single species. I analyze both mitochondrial (CO1, 16S) and nuclear (28S, H3) genetic data for 23 populations. Phylogeny for *H. barri* was reconstructed using both maximum-likelihood and Bayesian approaches to assess relationships among populations, and two species delimitation methods — mPTP and ABGD — were used to detect the presence of unique molecular operational taxonomic units (MOTUs). Species delimitation results revealed seven and sixteen MOTUs respectively, suggesting the presence of several cryptic lineages within *H. barri*. To assess how external shell morphology corresponds with both patterns of genetic and environmental variation, two morphometric approaches were utilized incorporating 115 shells from 31 populations. Both morphometric approaches reveal a significant environmental influence on shell morphology, and one approach showed the significance of MOTU groups. Further, I discuss the delimitation and morphometric results and additionally provide discussion on the taxonomic and conservation implications of this study.

TABLE OF CONTENTS

CHAPTER 1 INTRODUCTION	1
Undocumented Biodiversity within Subterranean Ecosystems	1
Influence of Geological and Climatic Processes on Subterranean Biodiversity	3
Morphological Disparity within Terrestrial Micromolluscs	4
Investigation Goals.....	8
CHAPTER 2 MATERIALS AND METHODS	9
Specimen Collection	9
DNA Extraction, Amplification, and Sequencing.....	14
Genetic Analyses.....	14
Phylogenetic Analyses and Species Delimitation	15
Morphometric Analyses	17
CHAPTER 3 RESULTS.....	22
Genetic Analyses.....	22
Phylogenetic Analyses	26
Species Delimitation	30
Morphometric Analyses	32
CHAPTER 4 DISCUSSION.....	36
Genetic Diversity of <i>Helicodiscus barri</i>	36
Utility of Shell Morphometrics in Species Delimitation of Cryptic Terrestrial Micromolluscs.....	41

Taxonomic and Conservation Implications.....	42
REFERENCES	44
APPENDIX.....	62
VITA.....	70

LIST OF TABLES

Table 1. <i>Helicodiscus barri</i> populations incorporated in this study, including 17 new populations. Cave names, Tennessee Cave Survey (TCS) cave number, county and state are provided, as well as information regarding which populations were considered in morphometric and genetic analyses.	10
Table 2. Summary statistics generated for all four genes assessed (mtDNA: CO1, 16S; nDNA: 28S, H3).	23
Table 3. Species delimitation results from both ABGD and mPTP analyses. Haplotype diversity, specimen ID, state, karst region, and physiographic province also included.	24
Table 4. Results from both TM and GM analyses. Asterisk (*) denotes significant p-values.....	35
Table A1. GenBank accession numbers for all sequence data.....	65
Table A2. <i>H. barri</i> CO1 sequence distance matrix generated for 16 cave populations (labeled by the respective Cave Survey number). Values in italics represent within group variation when this data is available.....	66
Table A3. <i>H. barri</i> 16S sequence distance matrix generated for 20 cave populations (labeled by the respective Cave Survey number). Values in italics represent within group variation when this data is available.....	67
Table A4. <i>H. barri</i> 28S sequence distance matrix generated for 21 cave populations (labeled by the respective Cave Survey number). Values in italics represent within group variation when this data is available.....	68

Table A5. *H. barri* H3 sequence distance matrix generated for 18 cave populations (labeled by the respective Cave Survey number). Values in italics represent within group variation when this data is available..... 69

LIST OF FIGURES

Figure 1. Photographs of <i>Helicodiscus</i> land snails, showing the white soft bodies and shell spiral lirae of both surface and cave-dwelling taxa. Top photo: <i>Helicodiscus barri</i> , photo credit: Matthew L. Niemiller. Bottom photo: <i>Helicodiscus lirellus</i> , photo credit: Ken Hotopp.	7
Figure 2. Geographic distribution of <i>Helicodiscus barri</i> from this study in relation to karst adapted from Weary and Doctor (2014). Triangles represent cave populations.	12
Figure 3. A: Entrance of Slippery Slit Cave. B: Entrance of McCoy Cave. C: Collection of <i>H. barri</i> on washed in decaying wood in Columbia Caverns (type locality). Photo Credits: Nicholas S. Gladstone.	13
Figure 4. A: Landmark scheme for geomorphometric analyses. Red circles represented landmarks (LM), blue circles represent semi-landmarks (SLM). B: Shell measurements utilized for the traditional morphometric (TM) analyses.	19
Figure 5. Haplotype network generated using the NeighborNet network method with uncorrected p-distances with the CO1 dataset. Species delimitation results are depicted using major color groups for the mPTP results, and subcolor groups for the ABGD results.	25
Figure 6. Phylogenetic tree of the CO1 dataset (808 bp) using the BI methodology. Posterior probabilities generated from the analysis are shown for each clade with the top numbers. Confidence values given from the bootstrapped ML method are shown for each clade with the bottom numbers. The 'x' symbols indicate varying topology between the BI and ML analyses. ML trees are reported in the Appendix for cross-reference. Species delimitation results are depicted using major color groups for the mPTP results (right brackets), and subcolor groups for the ABGD results (left brackets).	28

Figure 7. Phylogenetic trees of the concatenated mtDNA (CO1 + 16S; 1316 bp) and the full mtDNA + nDNA (CO1 + 16S + 28S + H3; 3040 bp) datasets. Posterior probabilities generated from the analyses are shown for each clade with the top numbers. Confidence values given from the bootstrapped ML method are shown for each clade with the bottom numbers. The ‘x’ symbols indicate varying topology between the BI and ML analyses. ML trees are reported in the Appendix for cross-reference. Species delimitation results are depicted using major color groups for the mPTP results, and subcolor groups for the ABGD results..... 29

Figure 8. ABGD species delimitation results. **A:** Recursive and initial partitions under varying prior intraspecific divergences. **B:** Frequency histogram of K2P pairwise divergences. 31

Figure 9. PCA results from both geometric morphometric (left) and traditional morphometric (right) analyses. A-B: Total morphometric dataset (n=65) grouped by physiographic province. C-D: Morphometric dataset with complimentary molecular data (n=39) grouped by MOTUs from the mPTP analysis..... 34

Figure 10. Geographic distribution of MOTUs generated from the mPTP delimitation method in relation to karst adapted from Weary and Doctor (2014). Triangles represent cave populations. The numbers associated with each unique color corresponds to the associated mPTP MOTUs found in Table 3. 40

Figure A1. CO1 (704 bp) phylogram of *H. barri* generated from RAxML. Outgroup not shown due to long branch length..... 63

Figure A2. mtDNA + nDNA (CO1 + 16S + 28S + H3; 3040 bp) phylogram generated of *H. barri* from RAxML. Outgroup not shown due to long branch length. 64

CHAPTER 1

INTRODUCTION

Undocumented Biodiversity within Subterranean Ecosystems

Caves provide a model system in which to study the evolutionary processes and historical factors related to biogeography and speciation (Juan et al. 2010). These systems, characterized by geographic isolation and relatively simple biological communities, are often viewed as analogous to oceanic islands (Culver and Pipan 2009). Strong selective pressures and the isolation of subterranean ecosystems can result in morphological stasis among otherwise genetically distinct species, largely due to the parallel evolution of these lineages (Niemi et al. 2012). Further, many troglobites (i.e., terrestrial cave-obligates) exhibit broad, mosaic distribution patterns which, in conjunction with this morphological stasis, often confound traditional means of delimitating species boundaries (Jochum et al. 2015). Thus, troglobites are ideal models to address fundamental questions in ecology and evolution and provide a platform to approach a more modernized integration of taxonomic methods.

Despite the relatively inhospitable conditions of subterranean environments (when compared to the surface), a taxonomically diverse fauna has been documented within the caves of the United States. Over 1,200 species have been documented, with many still awaiting formalized species descriptions (Hobbs 2012, Niemi et al. 2013). The Interior Low Plateau (ILP) and Appalachians karst regions are particularly species rich areas within the United States, exhibiting the first and second highest levels of North American troglobitic diversity, respectively (Culver et al. 2003). Karst regions are largely considered biodiversity hotspots (Myers et al. 2000), with

high levels of endemism associated with rock outcrops and caves (Clements et al. 2006). New molecular tools (e.g., environmental DNA sampling methods) are now being utilized to continue documenting biodiversity within these subterranean habitats (Niemiller et al. 2018), and increased awareness of the fragility of these systems is promoting cave conservation and management (Culver and Pipan 2009).

Phylogeography is the study of historical processes that have impacted the modern geographic distribution of species' populations by utilizing genetic data. Phylogeographic studies can provide a greater understanding of the importance of the hydrological and geological barriers that contribute to species diversification and how they shape biogeographic patterns (Avice 2000). The relative roles of vicariance and dispersal within subterranean ecosystems has been of increasing interest in light of continued advances in molecular biology and genomic methods (Porter et al. 2007; Culver et al. 2009; Juan et al. 2010). An increasing number of studies has investigated population genetic and phylogeographic hypotheses of subterranean fauna (e.g., Moulds et al. 2007; Snowman et al. 2010; Weckstein et al. 2016). Although conclusions have sometimes differed, these studies have greatly increased our understanding of colonization history, speciation, dispersal, and biogeography of troglobitic taxa (Juan et al. 2010). Regarding the conservation and management of such organisms, additional phylogeographic studies have uncovered considerable levels of cryptic species diversity (Finston et al. 2007; Juan and Emerson 2010; Niemiller et al. 2012). Due to increasing advances in imaging technology, studies that incorporate morphometric analyses often complement such molecular findings (Armbruster et al. 2016; Burrell et al. 2017; Jochum et al. 2015). The misidentification of species can hinder assessments of biodiversity and conservation of cryptic species. Therefore, an integrative

taxonomic evaluation of troglobitic taxa is needed to fully assess species richness within these systems, and to better inform their respective evolutionary histories. Moreover, cryptic species complexes may be comprised of groups already at significant risk of extinction (Niemiller et al. 2013).

Influence of Geological and Climatic Processes on Subterranean Biodiversity

The Interior Low Plateau (ILP) and Appalachians karst regions in North America are considerably biodiverse and cave-rich areas. Tennessee alone has over 10,000 documented caves, representing nearly 20% of all caves within the United States (Niemiller and Zigler 2013). Cave systems in eastern Tennessee are presumably more isolated due to the significant structural fragmentation of the Appalachians Ridge and Valley limestone by synclinal ridges of clastics, such as sandstone and shale. Conversely, limestones are exposed over larger areas within the Mississippian Plateaus in central Tennessee along the Highland Rim (Barr 1968). The discontinuity of Appalachians karst is largely supported by the high level of biological endemism, with many species being known from only a single cave (Christman et al. 2005; Niemiller and Zigler 2013). Troglobitic taxa within the ILP, on the other hand, have much greater dispersal potential, and have notably broader geographic distributions (Christman and Culver 2001; Niemiller and Zigler 2013).

Substantial climatic fluctuations during the Pleistocene have significantly influenced modern interpretations of biodiversity and the geographic distributions of species within North America (Webb III 1992). Many organisms were driven to extinction by unfavorable climatic conditions,

and others began transitioning to new niches which subsequently favored increased diversification (Hewitt 1996). Subterranean ecosystems are often considered important climatic refugia due to the relative stability of these systems. Many troglobitic taxa groups such as carabid beetles (Barr 1969), fishes (Niemiller et al. 2013), crayfishes (Buhay 2007), and arachnids (Bryson et al. 2014) are thought to be Pleistocene relicts (i.e., relict lineages of surface species driven to extinction following the Pleistocene), colonizing climatically stable subterranean habitats during periods of glacial advancement or recession. This aligns with the “Pleistocene-effect” model proposed by Holsinger (1988).

Morphological Disparity within Terrestrial Micromolluscs

Land snails (Phylum Mollusca, Class Gastropoda) are a significantly species-rich animal group. Over 24,000 species are currently recognized, and over 35,000 species are thought to exist globally (Barker 2001; Lydeard et al. 2004). The land snail fauna within eastern North America is exceptionally diverse, with over 500 species documented (Hubricht 1985; Nekola 2014). However, this likely represents an underestimate of total species richness in this region. Larger species are often associated with mesic forest ecosystems with high levels of moisture, leaf litter, and calcium (Goodfriend 1986; Pearce and Örstan 2006). Yet, land snails utilize a variety of microhabitats often neglected in sampling efforts within these areas (Cameron and Pokryszko 2005). Further, land snails occur at high density in karst-rich landscapes, and subterranean habitats are particularly under-sampled within the region (Clements et al. 2008; Niemiller and Zigler 2013).

Nearly 75% of all land snails in eastern North America are considered terrestrial micromolluscs (< 5 mm) and comprise a significant portion of all land snail diversity (Nekola 2005; Liew et al. 2008). Many of these species tend to be particularly under-sampled and often require the collection of soil and leaf litter samples to discover them (Liew et al. 2008; Nekola and Coles 2010; Durkan et al. 2013). Areas hypothesized to have comparatively higher levels of snail biodiversity have had varying and presumably insufficient collection efforts, with many cryptic species remaining unaccounted (Dourson 2007; Douglas et al. 2014; Dinkins and Dinkins 2018). This has led to a lack in the documentation of intraspecific morphological variation of micromolluscs, while also obscuring accurate geographic ranges for these species (Nekola and Coles 2010). Thus, as most land snail species are delimited on the basis of conchology (i.e., shell morphology), many collections sustain a high incidence of misidentification of minute species (Hubricht 1985; Nekola and Coles 2010), while also ignoring patterns of genetic variation. The continued misidentification of species can have significant impacts on biodiversity assessments and subsequent conservation management (Bickford et al. 2007).

Strictly utilizing morphological data to delimit extant species in the post-genomic era is often met with criticism (Hermsen and Hendricks 2008; Duminil and Di Michele 2009; Carstens et al. 2013). An integrative taxonomy (i.e., a combination of morphological, ecological, and genetic data when considering phylogenetic relationships) is necessary to facilitate proper interpretations of biological patterns (Dayrat 2005; Weigand et al. 2012). For gastropods, there are few discrete shell characters that can be used in phylogenetic hypotheses, and conchology is highly variable in response to environmental factors and other selective pressures (Goodfriend 1986; Smith and Hendricks 2013). However, morphometric analyses can contribute to species hypotheses when

combined with genetic data (Hermsen and Hendricks 2008; Miller 2016). Moreover, utilizing morphometric analyses can inform the causal mechanisms for shape variation between gastropod populations (Vergara et al. 2017).

Terrestrial micromolluscs of the genus *Helicodiscus* are found throughout the eastern United States (Hubricht 1985). This genus is markedly known for its unique conchological sculpture, often exhibiting depigmented soft bodies and prominent spiraling striae on the shells of both surface and subterranean species (**Figure 1**). Many of these species are calciphiles, and two species — *H. barri* Hubricht, 1962 and *H. notius specus* Hubricht, 1962 — have even adopted a cave-obligate existence (Hubricht 1962). The distributions of these troglobites span both the ILP and the Appalachians karst regions, covering multiple physiographic provinces within their ranges. The latter species is only known from six caves in Kentucky, Tennessee, and Virginia, whereas the former is known from 49 caves in Tennessee, Alabama, and Georgia. Two additional *Helicodiscus* species that were previously thought to be troglotic — *H. hadenoecus* and *H. punctatellus* — have recently been discovered at surface localities widely disjunct from their otherwise subterranean distribution (Coney et al. 1982; Hotopp et al. 2013). These distribution patterns suggest the potential for cryptic diversity within this genus among subterranean taxa. Further, morphological stasis is highly prevalent in troglobites despite significant genetic divergence, and, therefore, the mosaic distributions of these snails warrant investigation (Juan and Emerson 2010; Weigand et al. 2012).



Figure 1. Photographs of *Helicodiscus* land snails, showing the white soft bodies and shell spiral lirae of both surface and cave-dwelling taxa. Top photo: *Helicodiscus barri*, photo credit: Matthew L. Niemiller. Bottom photo: *Helicodiscus lirellus*, photo credit: Ken Hotopp.

Investigation Goals

In this project, I conduct the first study of the morphological variability and phylogeography of the cave-obligate land snail *Helicodiscus barri*. Recent cave bioinventory efforts within the ILP and Appalachians karst regions have allowed for the increased collection of the troglobitic species *Helicodiscus barri*. Other cave-dwelling *Helicodiscus* species have rarely been discovered (Hubricht 1962), and as such *H. barri* serves as the focal point of this investigation. This species is known from caves within both the Appalachians and ILP karst regions, across multiple established physiographic provinces. The disjunct, mosaic distribution pattern of *H. barri* in conjunction with a lack of clear morphological variation is consistent with a high potential for cryptic diversity. I examined museum accessions for *H. barri* while additionally sampling caves within the states of Tennessee, Alabama, and Georgia. Using phylogeographic approaches, I (1) assessed patterns of genetic variation (i.e., lasting gene flow, relative genetic similarity) of *H. barri* and employed two species delimitation methods (ABGD and mPTP) to infer the presence of cryptic lineages, and (2) tested if current species hypotheses based on conchology correspond with patterns of genetic variation. Further, I assessed morphological variation between *H. barri* populations using traditional morphometrics (TM) and landmark-based geometric morphometrics (GM).

CHAPTER 2 MATERIALS AND METHODS

Specimen Collection

Shell specimens were collected from 31 populations of cave-dwelling *Helicodiscus barri* from the dark zone of caves within both the ILP and Appalachian karst regions in Tennessee and Alabama (115 total individual specimens collected). Each survey typically involved two to four researchers (maximum 12), with a search effort of two to 36 person-hours per cave visit. In total, 74 caves were visited from 13 March 2013 to 19 June 2018 by NSG, totaling ca. 300 person-hours. Snail specimens were preserved in 100% ethanol and identified using published keys, species descriptions, and examination by taxonomic specialists (Pilsbry 1948; Hubricht 1962; Dourson 2010; Daniel Dourson, personal ID). Specimens from ten additional populations were provided by the Field Museum of Natural History (FMNH), Florida Museum of Natural History (FLMNH), and the Auburn Museum of Natural History (AUM). In all, 154 shells were examined (**Table 1**). The geographic distribution of populations utilized within this study can be found in **Figure 2**. Select sites are displayed in **Figure 3**.

Table 1. *Helicodiscus barri* populations incorporated in this study, including 17 new populations. Cave names, Tennessee Cave Survey (TCS) cave number, county and state are provided, as well as information regarding which populations were considered in morphometric and genetic analyses.

Label	Cave	TCS No.	County	State	References	n	Morphology	Genetic
NSG-DI3	Bowman Cave	TDI3	Dickson	TN	This study	2	X	X
NSG-KN112	Brents Cave	TKN112	Knox	TN	This study	3	X	X
AUM28348	Bull Run Cave	TDA4	Davidson	TN	Hubricht 1964	2	X	X
MLN 14-054.12; NSG-JK3	Carter Cave	TJK3	Jackson	TN	Gladstone et al. 2018	5	X	X
NSG-VB547	Cave Between the Caves	TVB547	Van Buren	TN	Lewis 2005	6	X	
NSG-RN5	Cave Creek Cave	TRN5	Roane	TN	This study	1		X
MLN 14-007	Christmas Cave	TDK72	DeKalb	TN	Gladstone et al. 2018	1	X	X
MLN 13-056	Clarksville Lake Cave	TMY11	Montgomery	TN	Gladstone et al. 2018	2	X	X
FMNH239117	Collier Cave	ALD100	Lauderdale	AL	Peck 1989	4	X	
FMNH239122; NSG-DI6	Columbia Caverns	TDI6	Dickson	TN	Hubricht 1962	7	X	X
NSG-KN50	Conner Creek Cave	TKN50	Knox	TN	This study	5	X	X
FMNH239121	Culbertson Cave	TUN22	Union	TN	Hubricht 1985	1	X	
NSG-AN5	Demarcus Cave	TAN5	Anderson	TN	This study	3		X
MLN 14-015.3	Dry Cave	TFR9	Franklin	TN	Gladstone et al. 2018	2		X
AUM27534-T2	Frazier Hollow Cave	DK11	DeKalb	TN	This study	1	X	X
NSG-DI27	East Fork Cave	TDI27	Dickson	TN	This study	2	X	
AUM28173	Hering Cave		Madison	AL	This study	1	X	X
NSG-FR14	Keith Cave	TFR14	Franklin	TN	Lewis 2005	10	X	X
UF 405128	Lady Finger Bluff Trail		Perry	TN	Gladstone et al. 2018	1	X	
WC13-165	Lovelady Cave	THM56	Hamilton	TN	This study	1		
NSG-MM10	McCorkle Cave	TMM10	McMinn	TN	This study	1		
NSG-VB9	McCoy Cave	TVB9	Van Buren	TN	This study	2	X	X

Table 1. Continued.

Label	Cave	TCS No.	County	State	References	n	Morphology	Genetic
AUM27855	New Salem Cave Nr1	TSM10	Smith	TN	This study	2	X	X
MLN 15-007.9	Oaks Cave	TUN5	Union	TN	Gladstone et al. 2018	1	X	X
FMNH305126; NSG-AN12	Offut Cave	TAN12	Anderson	TN	Hubricht 1985	8	X	X
MLN 15-006.19; NSG-CM8	Panther Cave No. 1	TCM8	Campbell	TN	Gladstone et al. 2018	7	X	X
FMNH239120	Parkers Cave	GKH119	Chattooga	GA	Holsinger and Peck (1971)	2	X	
NSG-KN108	Pedigo Cave Nr. 2	TKN108	Knox	TN	This study	1		X
NSG-AN6	Robert Smith Cave	TAN6	Anderson	TN	This study	2		X
MLN 13-000	Rockhouse Cave	ALM312	Limestone	AL	Gladstone et al. 2018	1	X	
AUM27652	Rogers Hollow Cave	TUN23	Union	TN	This study	2	X	
FMNH239118	Shelta Cave	AMD4	Madison	AL	Peck 1989	3	X	
NSG-OV440; GC1	Slippery Slit Cave	TOV440	Overton	TN	Lewis 2005	3	X	X
KSZ15-313	Smartt Farm Cave	GWK124	Walker	GA	This study	1		
NSG-VB657	Swamp River Cave	TVB657	Van Buren	TN	This study	1	X	
MLN-16.0228	Weavers Cave	TAN22	Anderson	TN	Gladstone et al. 2018	2	X	X
NSG-KN80	Wilke Waller Cave	TKN80	Knox	TN	This study	1		

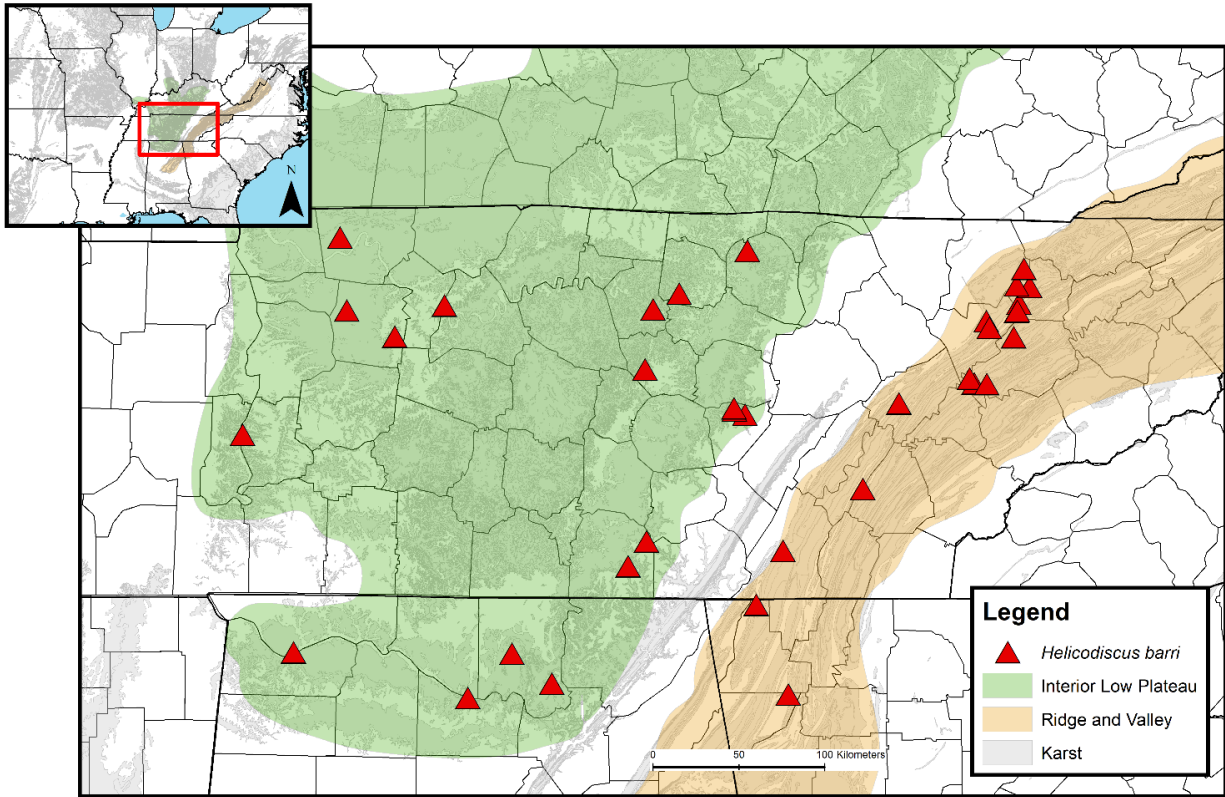


Figure 2. Geographic distribution of *Helicodiscus barri* from this study in relation to karst adapted from Weary and Doctor (2014). Triangles represent cave populations.



Figure 3. A: Entrance of Slippery Slit Cave. B: Entrance of McCoy Cave. C: Collection of *H. barri* on washed in decaying wood in Columbia Caverns (type locality). Photo Credits: Nicholas S. Gladstone.

DNA Extraction, Amplification, and Sequencing

Genomic DNA was obtained from soft tissue of each live specimen collected. The shells of smaller individuals were removed prior to DNA extraction. Tissue was removed from larger shells by breaking a small opening into the abapertural side of the shell or the shell base, so that the shell was not completely destroyed and remained identifiable. Each DNA extraction was performed using the Qiagen DNeasy Blood and Tissue kit following the manufacturer's protocol (Qiagen Sciences, Louisville, KY). Polymerase chain reaction (PCR) was used to amplify fragments of the mitochondrial (mt) 16S ribosomal RNA locus using the primer pair 16Sa/16Sb (Palumbi et al. 1991), the mt cytochrome oxidase subunit 1 (COI) locus using the primer pair LCOI490/ HCO2198 (Folmer et al. 1994), the nuclear 28S ribosomal RNA locus using the primer pair 28Sna1/28Sna2 (Kano et al. 2002), and the nuclear histone 3 (H3) locus using the primer pair H3F/H3R (Colgan et al. 2000). PCR products were purified using ExoSAP-IT (Affymetrix) and sequenced in both directions with BigDye chemistry at Eurofins MWG Operon (Huntsville, AL).

Genetic Analyses

Forward and reverse sequences were assembled into contigs and edited in Sequencher v.5.1 (Gene Codes Corporation). Alignments were modified by the manual trimming of the 3' and 5' primer ends. Ambiguous base calls and double peaks within heterozygotes were assessed visually with the chromatograms. Sequences were then aligned using MUSCLE under default parameters implemented in MEGA X v.10.0.5 (Kumar et al. 2018). All sequence data generated from this study were accessioned into GenBank (see **Table A1**). PartitionFinder v.2.1.1 (Lanfear

et al. 2012) was used to determine the best model for the sequence evolution for each partition based on the Bayesian information criterion (BIC). A general time-reversible model of sequence evolution with corrections for a discrete gamma distribution and a proportion of invariant sites (GTR+ Γ +I) was chosen for 16S. The Hasegawa, Kishino, and Yano (1985) model (HKY) with corrections for a discrete gamma distribution was chosen for the first and second codon positions of both CO1 and H3 as well as for 28S. A symmetrical model with corrections for a discrete gamma distribution (SYM+ Γ) was chosen for the third codon position of CO1 and H3 (Zharkikh 1994). Due to uneven coverage of genetic data across specimens, three unique *H. barri* datasets were assessed: CO1, *mtDNA* (CO1 + 16S), and *mtDNA* + *nDNA* (CO1 + 16S + 28S + H3). The species *Discus rotundatus* was used as an outgroup for all phylogenetic analyses. Summary statistics of the *H. barri* molecular dataset including haplotype and nucleotide diversity, number of segregating sites, haplotypes, and mutations were calculated in DnaSP v.6.12.01 (Librado and Rozas 2009). Uncorrected p-distances within and between cave populations were used as a metric of genetic divergence and calculated in MEGA X v.10.0.5 (Kumar et al. 2018). A haplotype network for all specimens for which genetic data were available was created in SplitsTree v.4.14.8 (Huson and Bryant 2005) using the NeighborNet network method with uncorrected p-distances.

Phylogenetic Analyses and Species Delimitation

Phylogenetic trees were inferred utilizing both a Maximum-Likelihood (ML) and Bayesian-inference (BI) approach. The ML analyses were conducted using RAxML v.8.0 (Stamatakis 2014) as implemented through the T-REX web server (Boc et al. 2012). A consensus tree was generated from the CO1, *mtDNA*, and *mtDNA* + *nDNA* datasets using rapid bootstraps for 100,000 replicates under a GTR+ Γ +I model of evolution. The BI analyses were conducted in

MrBayes v.3.2.6 (Ronquist et al. 2012) using a random start tree with three heated and one cold chain (default temperature of 0.1). This was run twice for 50,000,000 generations and sampled every 1,000 generations under the models of evolution determined by PartitionFinder. The first 25% of samples (12,500,000) were discarded as burn-in. Convergence of runs was assessed utilizing Tracer v. 1.4 (Rabaut and Drummond 2007).

The generation of molecular barcodes is often utilized in species delimitation in understudied groups (or in this case those that are morphologically ambiguous; Pons et al. 2006; Rubinoff 2006; Weigand et al. 2012, 2014). As such, two species delimitation approaches were subsequently used in the identification of Molecular Operational Taxonomic Units (MOTUs; Floyd et al. 2002): 1) Automatic Barcode Gap Recovery (ABGD; Puillandre et al. 2012), and 2) Multi-rate Poisson Tree Processes (mPTP; Kapli et al. 2017). ABGD partitions samples into candidate species based on a statistically inferred barcode gap. The barcoding gap is defined as a notable disparity between pairwise genetic distances, presumably between intraspecific and interspecific distances. This process is applied recursively to newly obtained groupings of sequences, to assess the possibility of internal division. This method will be carried out with the CO1 dataset excluding the outgroup (n = 24) via the ABGD web server (<http://wwwabi.snv.jusieu.fr/public/abgd/abgdweb.html>) using the Kimura two parameter (K2P; Kimura 1980) model with a standard X (relative gap width) = 1.5.

The initial development of PTP models assumed one exponential distribution for speciation events and one for all coalescent events (Zhang et al. 2013). In contrast, the mPTP approach fits

speciation events for each candidate species to a unique exponential distribution, greatly improving the quality of results (Kapli et al. 2017). This method requires a rooted phylogenetic tree and partitions samples into candidate species based upon the number of substitutions under assumed Poisson processes. Intraspecific substitution rates should be notably smaller than interspecific rates. This method does not require an ultrametric tree, which is ideal given little reliable fossil data for Helicodiscidae and the variability of molecular clock rates in Stylommatophoran gastropods (Thomaz et al. 1996; Chiba 1999; Van Riel et al. 2005). A rooted tree was generated for the CO1 dataset using the methods previously outlined for RAxML under the models of evolution determined by PartitionFinder. Analysis was carried out on the mPTP webserver (<http://mptp.h-its.org>) for the max 100,000 MCMC generations, with 25% of samples (25,000) conservatively discarded as burn-in.

Morphometric Analyses

Specimens were photographed using a Canon 6D digital camera while mounted on the Macropod PRO Micro Kit (Macroscopic Solutions, Tolland, CT). Each shell was photographed in three views: ventral, dorsal and apertural. MacroMagnification settings were extracted from the images using ExifTool v.5.16.0.0. Images were imported to Adobe Photoshop CS5 Extended v.12.1 and were subsequently scaled. Reproductive anatomy was not evaluated, given that most specimens were taken from museum collections with no soft tissue available. Two morphometrics methods were employed: geometric morphometrics (GM) and traditional morphometrics (TM).

GM techniques allow for the quantification and assessment of morphological variation. Biologically-meaningful landmarks (LMs) and semilandmarks (SLMs) of the *Helicodiscus* shells were digitized using tpsDig2 v. 2.32 (Rohlf 2015, available at <http://life.bio.sunysb.edu/morph/>). Nine homologous static LM were placed across each specimen. LM 1 is Type 1, characterizing the discrete juxtaposition of the homologous shell structure. LM 4 and LM 5 are Type 2, characterizing geometric maxima of curvature. All remaining LMs were Type 3, characterizing more than one region of each shell (Bookstein 1997). These eleven LMs were combined with two manually traced curves of three equidistant SLMs anchored on LM 4-5 and LM 5-6 (see **Figure 4A**). Appending tps curves to SLM was achieved using tpsUtil v. 1.76 (Rohlf 2015). This results in a total of nine fixed and six semi-landmarks.

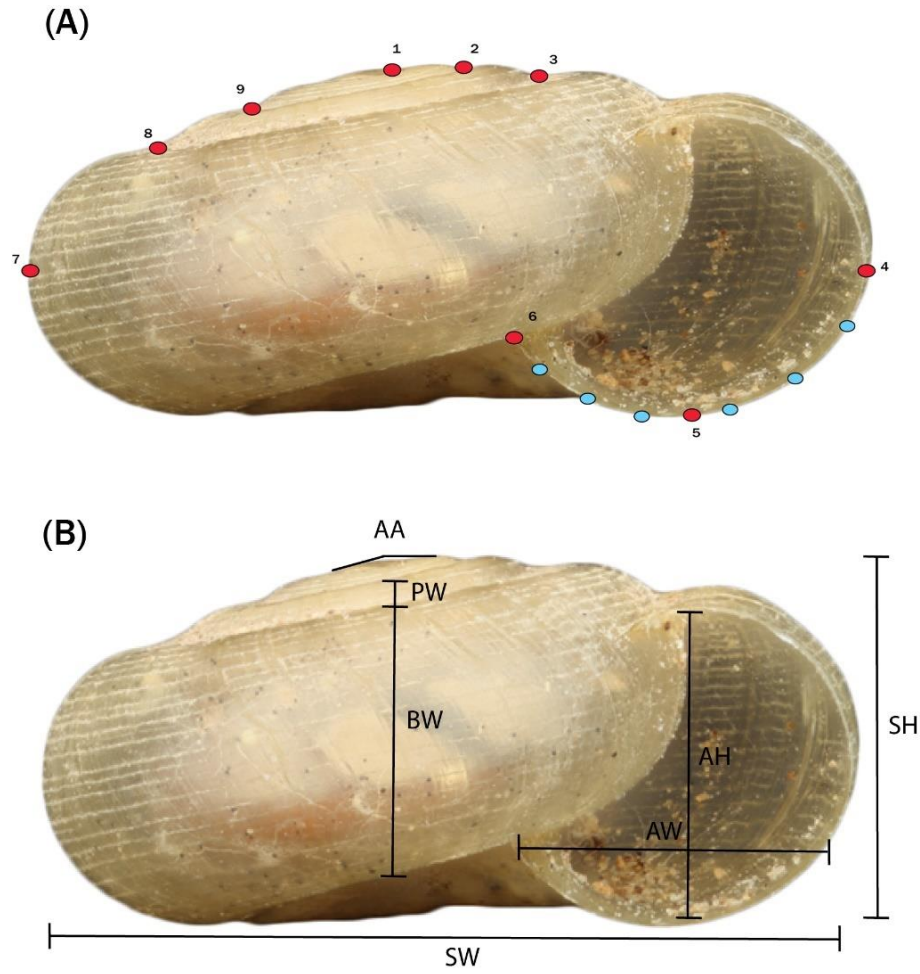


Figure 4. A: Landmark scheme for geomorphometric analyses. Red circles represented landmarks (LM), blue circles represent semi-landmarks (SLM). B: Shell measurements utilized for the traditional morphometric (TM) analyses.

To eliminate variation due to orientation of the shell or size, a Procrustes superimposition was performed using the *geomorph* package v.2.0. in RStudio v 1.1.456 with R v. 3.5 (Adams et al. 2013, 2014; RC Team 2014). These data were subjected to principal component analysis (PCA) to evaluate the distribution of populations in morphospace. Several alternative landmark schemes were tested but provided no notable differences in PCA results. The most conservative approach was utilized to reduce the number of variables introduced into the downstream analyses. Correlation coefficients (PC loadings) of individual variables were assessed visually to determine which specific variables are significant to each PC as to interpret what shell characteristics account for variability of the data set. To quantify error associated with landmark placement and shell placement during photography, a set of replicate images with digitized landmarks was used to calculate the disparity using the *morphol.disparity* function in *geomorph* (Adams et al. 2013, 2014).

Specimens were grouped by MOTUs to identify detectable differences in shell variation in concordance with genetic variation. Reduced datasets of those specimens with obtained genetic data were used for these groups. However, in the absence of genetic data, all specimens for which data are available were grouped by the physiographic province associated with the collection locality (i.e., Cumberland Plateau, Eastern Highland Rim, Valley and Ridge, and Western Highland Rim). These regions possess unique environmental characteristics (Fenneman 1917) and were utilized as broad-scale categories to test for the effect of environmental variation on conchology. Before assessing the significance of these groups in explaining morphological variation, the first and second PCs were subjected to a test of spatial autocorrelation (SAC) to prevent the increase of Type 1 errors introduced to the analyses (Perez et al. 2010). SAC was

determined using the Moran's I statistic (Sokal and Oden 1978) and was found to be non-significant (PC 1=0.2184, PC 2=0.0832). These groups will be subject to Procrustes Analysis of Variance (ANOVA) following a randomized residual permutation procedure (RRPP) for 10,000 iterations.

Seven unique shell measurements from Burch (1962) were utilized in the TM approach (see **Figure 4B**): Shell width (SW), shell height (SH), aperture width (AW), aperture height (AH), body whorl height (BW), penultimate whorl height (PW), and angle of apex (AA). These shell characteristics are often utilized in morphometric analyses and are readily utilized in land snail species' identification (Pearce and Örstan 2006, Dourson 2010). Scaled data were converted to a Euclidean distance matrix and subject to Permutational Multivariate Analysis of Variance (PERMANOVA). This was performed in the *vegan* package in R for 10,000 permutations (Oksanen 2018). *P*-values extracted from pairwise comparisons were corrected using a Bonferroni test.

CHAPTER 3 RESULTS

Genetic Analyses

Molecular sequence data were obtained from 32 specimens of 23 populations. Tissue samples were scarce, and the saturation of the land snail soft body with mucopolysaccharides inhibits the success of standard extraction procedures and subsequent sequencing. Thus, I was unable to obtain full genetic coverage (i.e., all four target genes sequenced) for all specimens. Summary statistics generated for the genetic data can be found in **Table 2**. The *mtDNA* dataset used for the gene tree estimation was unambiguously aligned (1316 base pairs; bp). A concatenated alignment of all specimens in which all four genes were amplified was also unambiguously aligned and assessed (n = 16; 3040 bp). The CO1 dataset was also assessed independently, as it was later utilized for the downstream species delimitation approaches. The CO1 data were unambiguously aligned (n=24; 704 bp). No shared haplotypes were observed between cave populations at CO1 (see **Table 3**), even in cases where caves were less than 15 m apart from one another (e.g., Demarcus Cave and Robert Smith Cave). The generated haplotype network strongly resembles MOTU delimitation results (**Figure 5**), with the two most diverse MOTUs identified possessing five haplotypes each. Mean uncorrected p-distances between cave populations at CO1 was 16.14% (range 2.6% – 23.2%), indicating significant geographic isolation. For the concatenated genetic dataset, mean uncorrected p-distances between cave populations was 6% (range 1.3% – 10.3%). Due to the rarity of this species, there were only four instances of obtaining sequences of more than one individual per cave (Columbia Caverns, Keith Cave, Offut Cave, Panther Cave No. 1). Of these, two populations exhibited two haplotypes at

Table 2. Summary statistics generated for all four genes assessed (*mtDNA*: CO1, 16S; *nDNA*: 28S, H3).

	<i>n</i>	<i>bp</i>	<i>h</i>	<i>Hd</i>	<i>Π</i>	<i>S</i>	<i>Eta</i>
<i>mtDNA</i>							
CO1	24	668	18	0.957 ± 0.031	0.14346 ± 0.012	164	245
16S	28	605	20	0.968 ± 0.019	0.09019 ± 0.011	71	99
<i>nDNA</i>							
28S	29	1305	6	0.424 ± 0.111	0.00327 ± 0.001	20	20
H3	25	337	6	0.427 ± 0.122	0.00322 ± 0.001	7	7

n — number of sequences

bp — alignment size

h — number of haplotypes

Hd — haplotype diversity

Π — nucleotide diversity

S — number of polymorphic sites

Eta — number of mutations

Table 3. Species delimitation results from both ABGD and mPTP analyses. Haplotype diversity, specimen ID, state, karst region, and physiographic province also included.

mPTP	ABGD	Haplotype ID	Specimen ID	State	Karst	Physiographic
PG1	AG1	H1, H2	NSG-CM8-T1, NSG-CM8-T2, MLN-15-006.19	TN	APP	VR
PG2	AG2	H3	NSG-AN12-T1, NSG-AN12-T2, NSG-AN12-T3, NSG-AN12-T4, NSG-AN12-T5	TN	APP	VR
PG3	AG3, AG4, AG5, AG6, AG7	H4, H5, H6, H7, H8	NSG-JK3-T1, NSG-VB9-LL, GC1, NSG-DI3-LL, NSG-FR14-T1, NSG-FR14-T2	TN	ILP	CP, EHR, WHR
PG4	AG8	H9	NSG-AN5-NP	TN	APP	VR
PG5	AG9	H10	MLN-14-0153	TN	ILP	CP, EHR
PG6	AG10, AG11, AG12 AG13,	H11, H12, H13	AUM27534-T2, NSG-KN50-NP, NSG-AN6-NP	TN	APP, ILP	VR, WHR
PG7	AG14, AG15, AG16	H14, H15, H16, H17, H18	MLN-16.0228, NSG-KN112-T1, NSG-DI6-T1, NSG-DI6-T2, AUM28173	AL, TN	APP, ILP	CP, VR, WHR

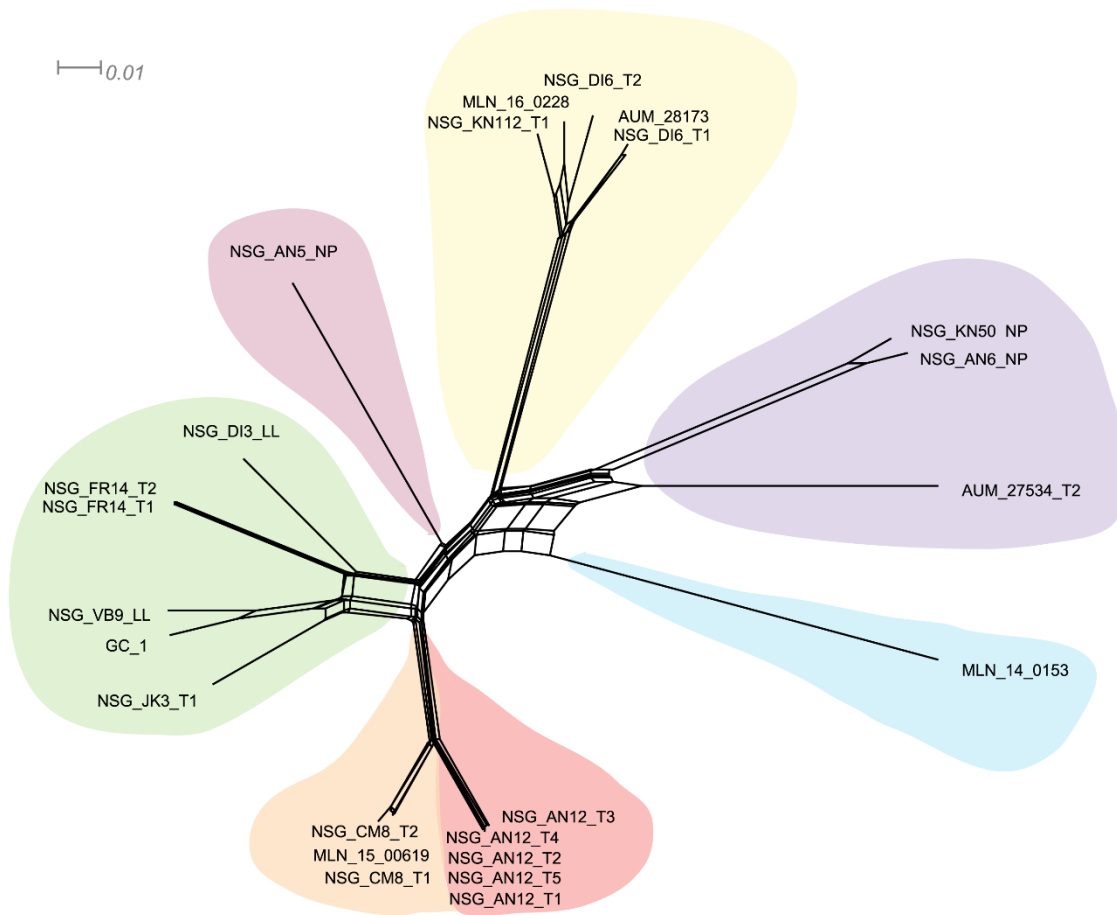


Figure 5. Haplotype network generated using the NeighborNet network method with uncorrected p-distances with the CO1 dataset. Species delimitation results are depicted using major color groups for the mPTP results, and subcolor groups for the ABGD results.

CO1. Intrapopulation variation of these four populations was low, with a mean CO1 uncorrected p-distance of 1.48%.

Phylogenetic Analyses

Both ML and BI approaches resulted in highly similar tree topologies for each unique concatenated genetic dataset (CO1, *mtDNA*, *mtDNA* + *nDNA*). The outstanding difference between the ML and BI phylograms generated from the *mtDNA* dataset was a resolution of polytomy from the ML approach in the Bowman Cave (DI3), Carter Cave (JK3), Keith Cave (FR14), McCoy Cave (VB9), and Slippery Slit Cave (OV440) clade. The *mtDNA* + *nDNA* phylograms also differed with the Hering Cave (AMD6) population representing a monotypic group in the ML approach, and grouping with the Brent's Cave (KN112), Columbia Caverns (DI6), and Weavers Cave (AN22) clade as it does in all other phylograms assessed. Additionally, there were several notable distinctions in the CO1 phylograms produced between BI and ML approaches (see **Figure A1**). Despite these differences, only the representative phylogenies utilizing the BI approach for the CO1, *mtDNA*, and *mtDNA* + *nDNA* datasets are shown in **Figure 6, 7**. All other trees are placed within the Appendix (**Figure A1-A2**).

Due to an inability to amplify all genes per specimen, some specimens are not represented in all phylogenies. However, among the representatives included in all three datasets, there is a consistent topology. The only differences between the *mtDNA* tree and the *mtDNA* + *nDNA* BI trees are 1.) the resolution of polytomy and varied topology in the Bowman Cave (DI3), Carter

Cave (JK3), Keith Cave (FR14), McCoy Cave (VB9), Slippery Slit Cave (OV440) clade, and 2.)
the relative placement of the Frazier Hollow Cave (DK11), Robert Smith Cave (AN6), and
Conner's Creek Cave (KN50) clade. All other clades remain consistent. Confidence values for

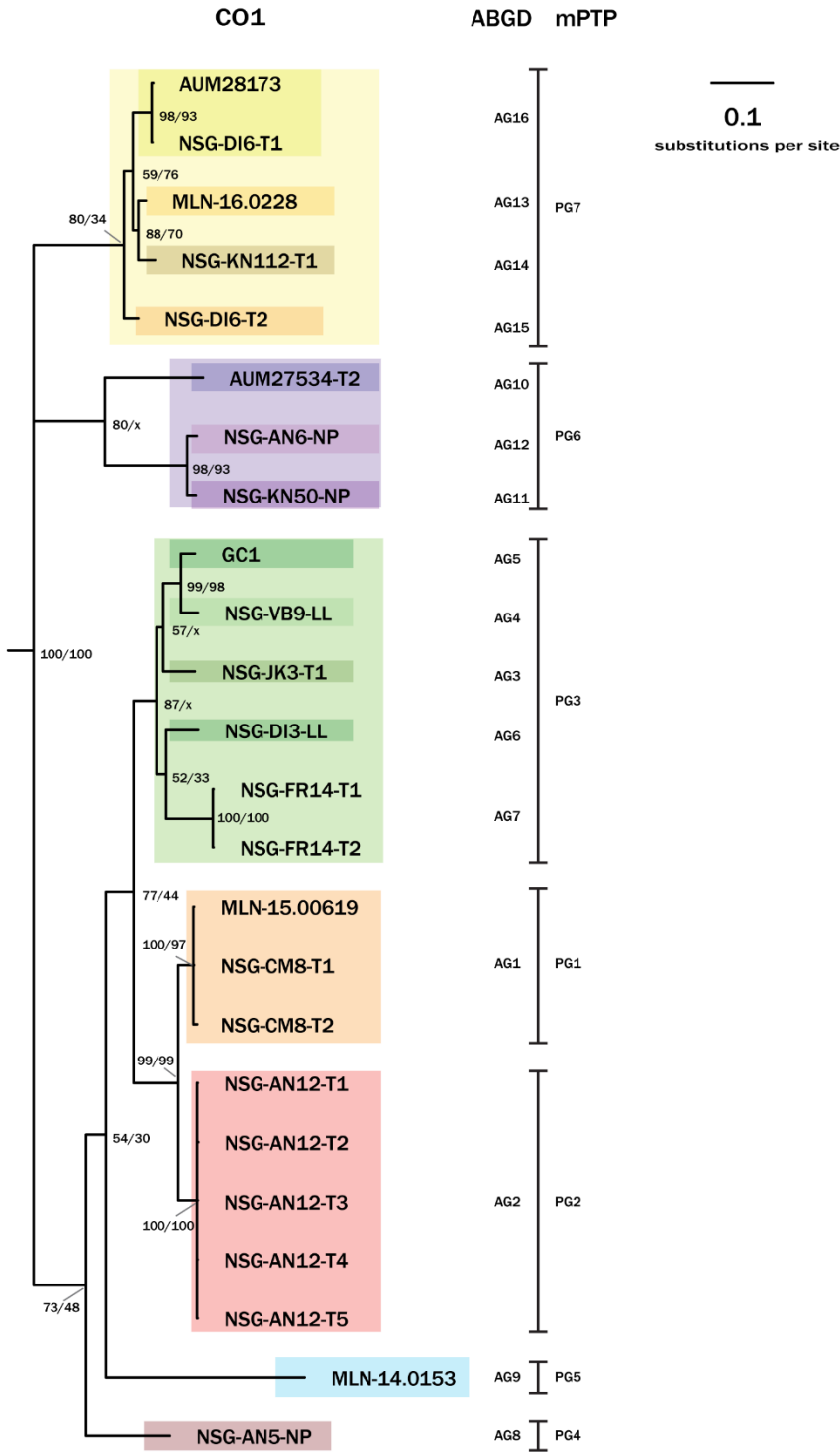


Figure 6. Phylogenetic tree of the CO1 dataset (808 bp) using the BI methodology. Posterior probabilities generated from the analysis are shown for each clade with the top numbers. Confidence values given from the bootstrapped ML method are shown for each clade with the bottom numbers. The ‘x’ symbols indicate varying topology between the BI and ML analyses. ML trees are reported in the Appendix for cross-reference. Species delimitation results are depicted using major color groups for the mPTP results (right brackets), and subcolor groups for the ABGD results (left brackets).

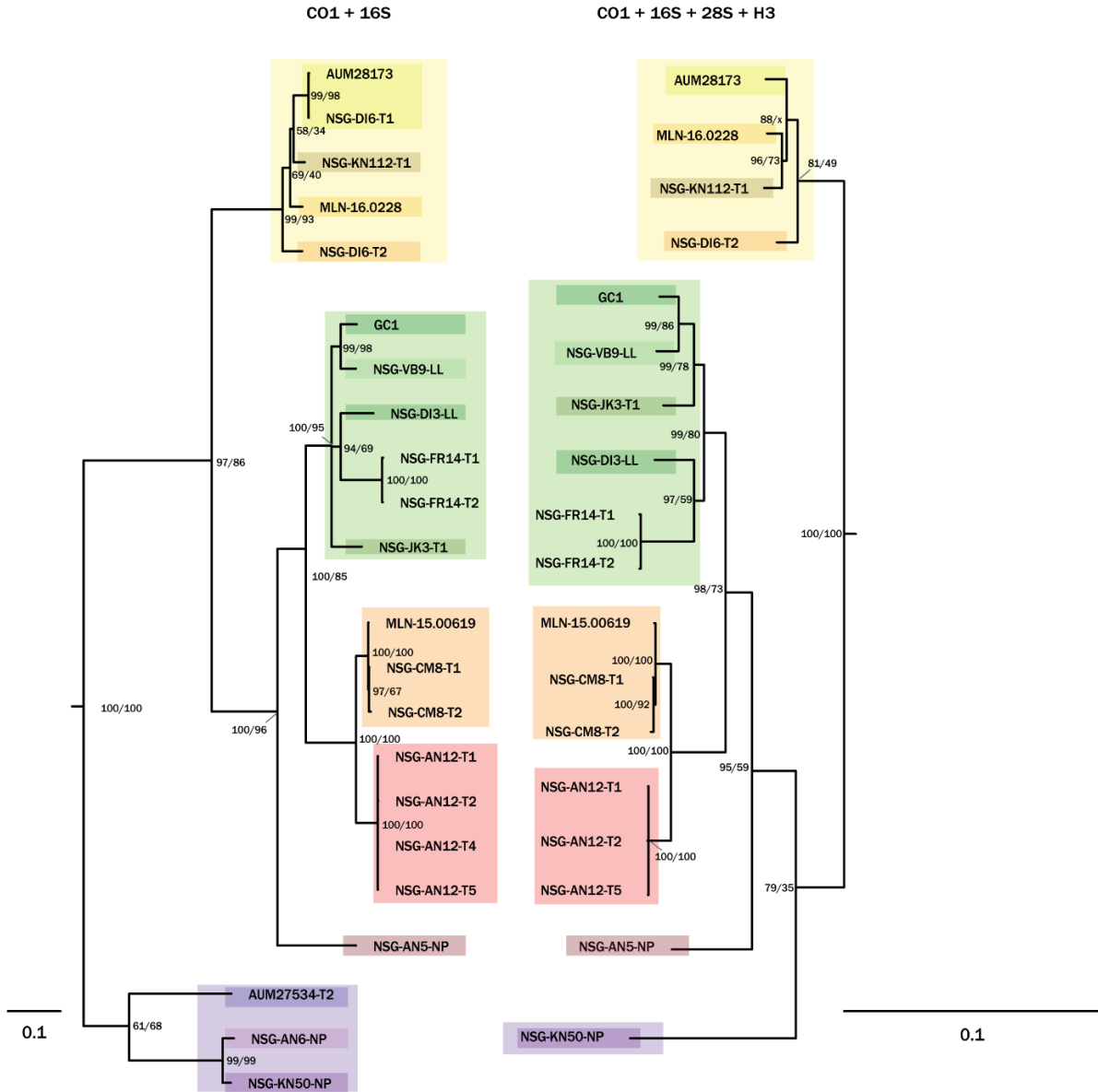


Figure 7. Phylogenetic trees of the concatenated *mtDNA* (COI + 16S; 1316 bp) and the full *mtDNA* + *nDNA* (COI + 16S + 28S + H3; 3040 bp) datasets. Posterior probabilities generated from the analyses are shown for each clade with the top numbers. Confidence values given from the bootstrapped ML method are shown for each clade with the bottom numbers. The ‘x’ symbols indicate varying topology between the BI and ML analyses. ML trees are reported in the Appendix for cross-reference. Species delimitation results are depicted using major color groups for the mPTP results, and subcolor groups for the ABGD results.

the ML approach were notably lower at deeper nodes in each phylogram, and the same occurred with posterior probabilities generated from the BI approach. Node posterior probabilities and confidence values increased overall after the addition of the *nDNA* data. Comparison of both *mtDNA* and *nDNA* phylograms show the existence of at least seven monophyletic clades across the Appalachians and ILP karst regions. The monotypic Dry Cave (FR9) and Demarcus Cave (AN5) clades seem to be considerably divergent from other groups. While the former is known from the southern extent of the Eastern Highland Rim, the latter monotypic clade is located in immediate proximity to Robert Smith Cave (less than 15 m) yet are significantly delineated in the CO1 phylogram and the subsequent delimitation approaches.

Species Delimitation

The ABGD method generated two partition strategies. At prior intraspecific divergence (P) values between 0.0010 and 0.0215, sixteen MOTUs were recognized in initial and recursive partitions (see **Figure 8A**). Both partition schemes remained stable at these values until reaching congruency at $P = 0.0359$, grouping all populations together into a single MOTU. The barcode gap was discovered at 0.14-0.16 K2P distance (see **Figure 8B**). The PTP results generated seven MOTUs for both single and multi-coalescent rate models. Both delimitation approaches show highly similar MOTU designations, with most identified groups being known from individual caves. There were four cases of both delimitations methods producing the same results (PG1, PG2, PG4, PG5). Three groups of five, four, and three MOTUs generated by ABGD were grouped were consolidated into three MOTUs generated by mPTP (PG3, PG6, PG7), respectively. The consolidated PG3 MOTU group is largely clustered within the Eastern Highland Rim (AG3, AG4, AG5, AG7), with only one disjunct representative being found in a

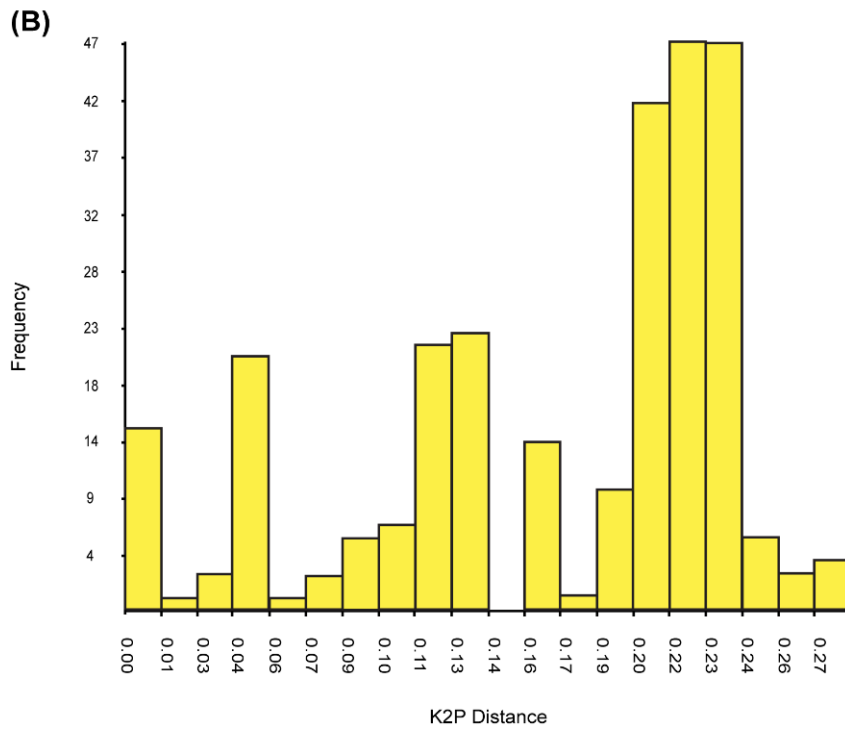
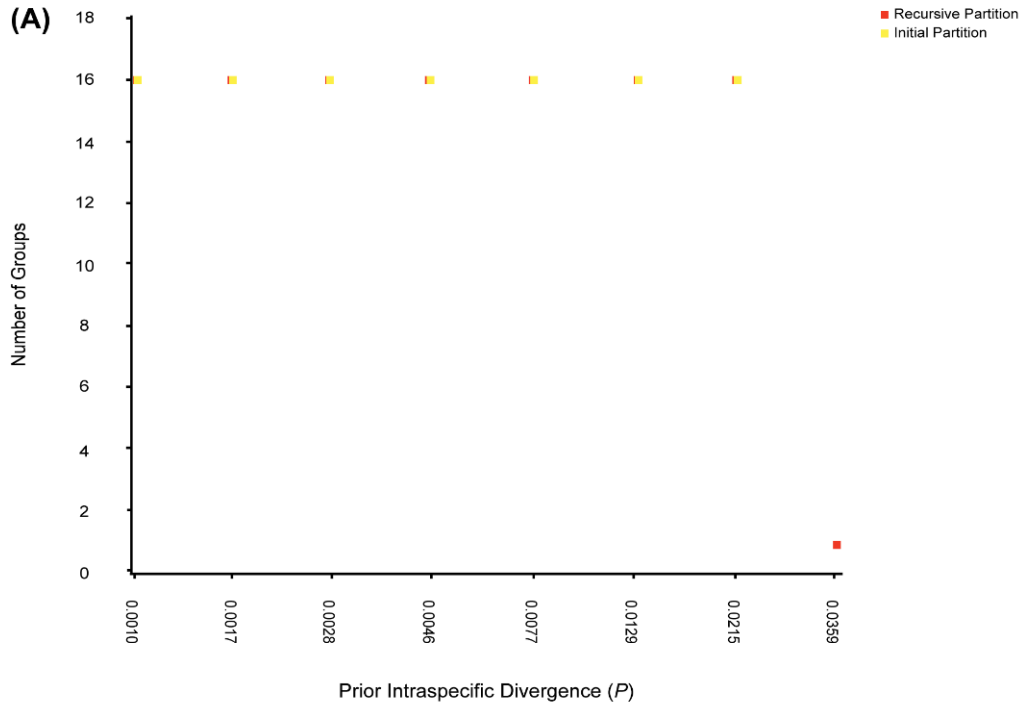


Figure 8. ABGD species delimitation results. **A:** Recursive and initial partitions under varying prior intraspecific divergences. **B:** Frequency histogram of K2P pairwise divergences.

fragmented karst formation on the eastern extent of the Western Highland Rim (AG6). The PG6 and PG7 MOTU groups exhibit an irregular geographic structure, with both possessing representatives from both karst regions (Appalachians and ILP). Further, the ABGD results suggest two MOTU groups (AG15, AG16) within a single cave population at Columbia Caverns, with AG16 comprising this cave on the eastern extent of the Western Highland Rim and another in the southern extent of the Cumberland Plateau in the state of Alabama.

Morphometric Analyses

In total, 65 individuals were incorporated into both the GM and TM datasets from 28 cave populations. The disparity test used to indicate possible error introduced from shell and landmark placement (2.28%) was negligible. For the GM PCA, the first three principal components account for 69.52% of the total variance. PC 1 (31.24%) was interpreted as the curvature of the shell, with higher PC scores exhibiting a higher angle of apex and larger shell height. The X-coordinates of LM 3, LM 2, and LM 6 all had the highest PC loadings associated with PC 1 (0.418, 0.312, 0.243 respectively). PC 2 (25.18%) was interpreted as the size of the secondary body whorl in relation to the aperture, with higher PC scores exhibiting significantly wider secondary body whorls with an annular apertural structure. The Y-coordinate of LM 8 and the X-coordinates of LM 9 and LM 1 had the highest PC loadings associated with PC 2 (0.281, 0.189, 0.159 respectively). PC 3 (13.10%) was interpreted as the size of the aperture, with higher PC scores exhibiting larger apertures and higher shell width. The X-coordinates of LM 6 and SLM 15 and the Y-coordinate of LM 4 had the highest PC loadings associated with PC 3 (0.354, 0.333, 0.301 respectively). A smaller morphometric dataset ($n = 39$) was assessed for those

individuals for which molecular data was available. Only the MOTU groups from the mPTP analysis were considered, as these were the larger groups. The first three principal components for this smaller dataset account for 74.90% of the total variance (PC 1 = 31.03%; PC 2 = 28.76%; PC 3 = 15.11%). PC plots for each grouping are displayed in **Figure 9A-D**.

For the TM PCA, the first three principal components accounted for 79.36% of the total variance. PC 1 (66.03%) was interpreted as the overall size of the shell, with high PC scores exhibiting larger shell height and shell width (PC loadings = 0.4553, 0.4370 respectively). PC 2 (13.23%) was interpreted as the height of the shell, with higher PC scores exhibiting much larger penultimate whorls and shell height (PC loadings = 0.6336, 0.6011 respectively). PC 3 (9.85%) was interpreted as the curvature of the shell, with higher PC scores having higher angles of apex and smaller shell width (PC loadings = 0.6815). For the smaller mPTP dataset, the first three principal components accounted for 85.98% of the total variance. Procrustes ANOVA and PERMANOVA testing the influence of environmental variation (i.e., respective physiographic province) on external shell morphology indicated significance for both morphometric approaches. MOTU groups did not significantly explain shell variation with the GM approach, but it was significant for the TM approach (**Table 4**).

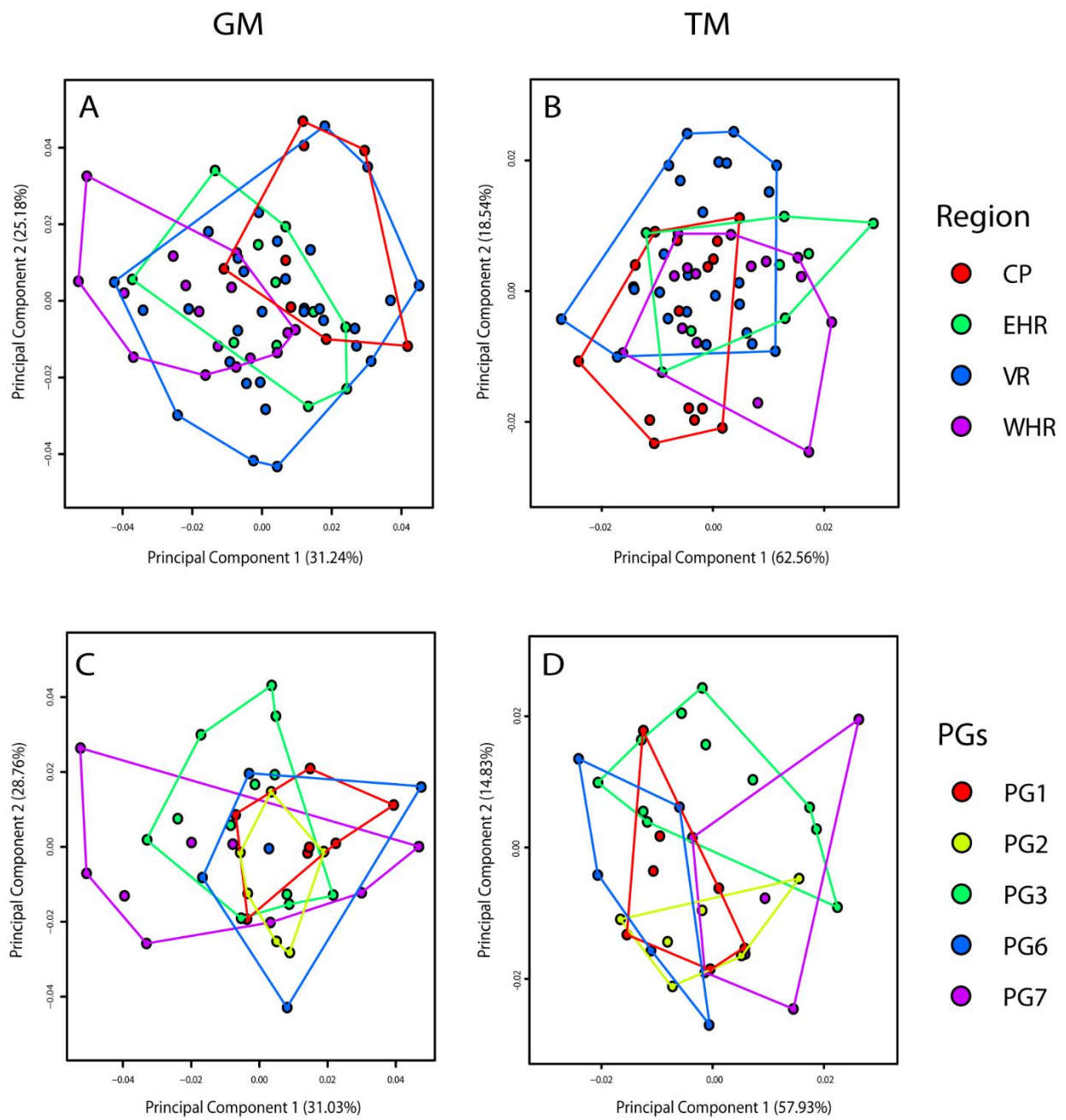


Figure 9. PCA results from both geometric morphometric (left) and traditional morphometric (right) analyses. A-B: Total morphometric dataset (n=65) grouped by physiographic province. C-D: Morphometric dataset with complimentary molecular data (n=39) grouped by MOTUs from the mPTP analysis.

Table 4. Results from both TM and GM analyses. Asterisk (*) denotes significant p-values.

Procrustes ANOVA					
Group	Degrees of Freedom	Sums of Squares	R ²	<i>F</i>	<i>P</i>
MOTUs (mPTP)	4	0.00763	0.14037	1.388	0.1311
Physiographic Province	3	0.01291	0.13503	3.1742	2.00E-04*

Permutational MANOVA					
Group	Degrees of Freedom	Sums of Squares	R ²	<i>F</i>	<i>P</i>
MOTUs (mPTP)	4	80.084	0.30107	3.6614	3.00E-04*
Physiographic Province	3	69.84	0.15589	3.7553	0.0021*

CHAPTER 4 DISCUSSION

Many molecular studies of troglobitic taxa have discovered previously unknown cryptic lineages in North America (Buhay and Crandall 2009; Snowman et al. 2010; Niemiller et al. 2012; Weckstein et al. 2016). Troglobites are thought to have fewer opportunities for dispersal than obligately-subterranean aquatic species (i.e., stygobites), due to limited connectivity of terrestrial subterranean passages. This may promote isolation and short-range endemism in troglobites (Culver et al. 2009; Niemiller and Zigler 2013). No phylogeographic study of troglobitic snails has been conducted in North America, and all other molecular studies of troglobites in the Appalachians and Interior Low Plateau have focused on organisms with comparatively higher vagility and dispersal potential (e.g., Buhay et al. 2007; Niemiller et al. 2008; Niemiller et al. 2011; Snowman et al. 2010; Loria et al. 2011). Using both a multilocus molecular and morphometrics approaches, my goal for this study was to investigate genetic diversity within *H. barri* to potentially identify cryptic populations within the species' range, and to further determine whether external shell morphology was a useful indicator of differing patterns of genetic variation.

Genetic Diversity of *Helicodiscus barri*

Despite limited sampling success of this rare species, this study revealed high genetic diversity in *H. barri*. Haplotypic diversity is strongly dictated by individual caves, and there appears to be little to no dispersal between cave systems regardless of proximity. Mitochondrial genetic divergence among *H. barri* populations is significantly higher (16.14%) compared to other

troglobitic invertebrate taxa (e.g., 3.1% for *Nesticus* spiders; Snowman et al. 2010; 0.06% for *Tetracion* millipedes; Loria et al. 2011; 2.1% for *Ptomaphagus* beetles; Leray et al. 2019), suggesting that the low vagility of land snails accentuates the isolation caused by subsurface habitat fragmentation. Rates of mitochondrial gene evolution for land snails vary considerably, with estimates of 1.6%-12.9% per million years for ribosomal genes and 2.8%-13% for CO1 (Thomaz et al. 1996; Chiba 1999; Van Riel et al. 2005). Further, intraspecific population structure is known to exhibit high genetic divergence (Guiller et al. 1994; Davison et al. 2009; Perez et al. 2014). An estimated 1.6% divergence per million years has been a proposed standard for other gastropods (Liu and Hershler 2007; Murphy et al. 2012; Harris et al. 2013). With this conservative estimate, CO1 sequence divergence suggests the average timing of isolation between *H. barri* populations is 10.1 million years, and up to 14.5 million years. In this scenario, not only do these results indicate the evolutionary independence of these cave populations, they suggest that the subterranean colonization of this species pre-dates the Pleistocene glaciation. The Climatic Relict Hypothesis, which suggests that environmental stress (such as the often implicated Holsinger (1988) “Pleistocene-effect” model) drives the colonization of organisms into subterranean environments (Leys et al. 2003; Culver and Pipan 2009). This scenario rejects this hypothesis, and instead favor a scenario in which a geographically widespread proto-troglobitic (i.e., troglomorphic) species colonized different subterranean systems independent of obvious environmental stress.

Mitochondrial divergence estimates of $\geq 10\%$ per million years are, however, often associated with terrestrial gastropods on island systems (Chiba 1996; Thacker and Hadfield 2000; Van Riel et al. 2005), which are highly comparable to cave systems due to the isolation of subterranean

environments and the discontinuity of these habitats across karst landscapes (Culver 1970; Snowman et al. 2010). In this latter scenario of a high rate of mitochondrial gene evolution (10% per million years), average timing of isolation is 1.6 million years. This would suggest a climatically-driven subterranean colonization during the mid-Pleistocene, failing to reject the Climatic Relict Hypothesis. Thus, it is difficult to infer an accurate scenario without the application of a *Helicodiscus*-specific molecular clock model. However, the development of an accurate molecular clock is problematic due to a notable gap in fossil material for the genus in North America. There are several occurrences of fossil material in surface and cave habitats across central and eastern North America during the Pleistocene (Rinker 1949; Wetmore 1962; Slaughter 1966; Schultz and Cheatum 1970; Guilday et al. 1977; Dalquest and Stangl 1984; Eshelman and Hager 1984), and one fossil record in central North America in the upper Miocene (Liggert 1997). Moreover, dating on the basis of biogeographic barrier formation is also problematic, as timing estimates of cave formation across the distribution of *H. barri* are highly variable. The formation of some caves in the eastern Appalachians and Cumberland Plateau have been estimated to occur in the late Pliocene to middle Pleistocene (Davies 1953; Anthony and Granger 2004; White 2009), while other caves along the Tennessee River Valley and the Highland Rim have been estimated to form in the late Mesozoic to the early Tertiary (Moneymaker 1948; Barr 1961). Therefore, assessing the timing of colonization is currently beyond the scope of this study.

Delimitation results reveal up to sixteen unique MOTUs within *H. barri*, largely organized by geographic and geological similarity (see **Figure 10**). Most MOTUs belong to similar rock groups, arranged largely in association with each respective physiographic province. There were

two unique cases of MOTUs being distributed across both the Appalachians and ILP karst, each exhibiting irregular geographic structure. PG7 is distributed across four cave populations from the northeastern Valley and Ridge, the southernmost contact zone of the Cumberland Plateau and the Eastern Highland Rim, and the westernmost extent of the Western Highland Rim. PG6 is distributed across three cave populations in the eastern Central Basin and the northeastern Valley and Ridge. Further, the ABGD results reveal two distinct MOTUs (AG15, AG16) within a single cave population at Columbia Caverns (DI6). AG15 is comprised of a single individual from Columbia Caverns, whereas AG16 is comprised of one individual from Columbia Caverns and another from the Hering Cave population in northern Alabama. This pattern may be the product of multiple cave colonization events in Columbia Caverns, or perhaps this demonstrates a case of sympatric speciation as a consequence of niche partitioning (e.g., Cooper et al. 2002; Niemiller et al. 2008), as these individuals were found in two separate areas of this large cave system. However, due to a low sample size, the aforementioned limited fossil data, and the uncertainty in estimating biogeographic barrier formation, it is difficult to determine the evolutionary history of this species and the geologic context whereby these unique MOTU groups may have developed.

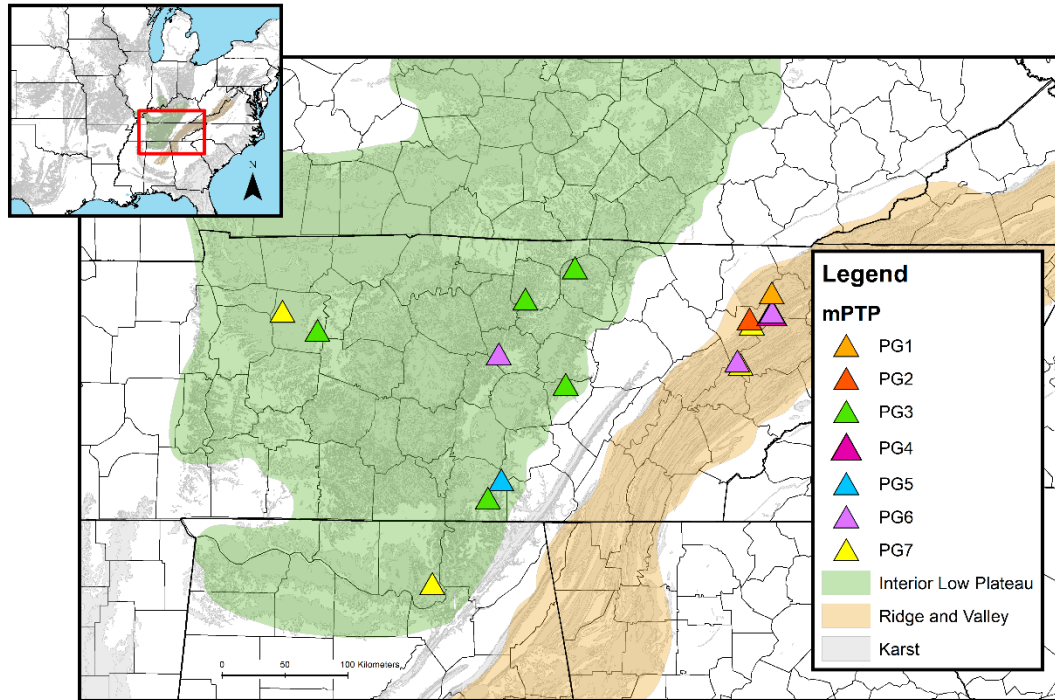


Figure 10. Geographic distribution of MOTUs generated from the mPTP delimitation method in relation to karst adapted from Weary and Doctor (2014). Triangles represent cave populations. The numbers associated with each unique color corresponds to the associated mPTP MOTUs found in Table 3.

Utility of Shell Morphometrics in Species Delimitation of Cryptic Terrestrial Micromolluscs

There has been much debate regarding the use of gastropod shell morphology in phylogenetic analyses (Emberton 1995; Wagner 2001; Uit de Weerd 2004; Smith and Hendricks 2013; Miller 2016). Shell variation, while informative at lower taxonomic resolutions (e.g., Smith and Hendricks 2013), may not be useful in accurate delimitation of cryptic lineages, owing to the high responsiveness of shell structure to environmental factors and commonality of local adaptations in land snails (Goodfriend 1986; Fiorentino et al. 2008; Stankowski 2011; Razkin et al. 2017). Moreover, though many subterranean taxa (here including *Helicodiscus barri*) exhibit disjunct, fragmented distributions, the ecological similarity of subterranean environments can lead to the protraction of morphological distinguishability between distinct genetic lineages (Losos and Mahler 2010; Eme et al. 2018). Terrestrial micromolluscs pose additional difficulty in morphological delimitation due to their small size and similarities in external shell morphology, and molecular approaches have been favored (e.g., Weigand et al. 2012). Recent study of troglobitic *Zospeum* snails show that external shell morphology shows high variability both within and between cave populations, further obscuring the taxonomic identity of these cryptic groups without molecular data and intensive study of internal shell structure and soft tissue histology (Jochum et al. 2015).

Results herein indicate geographic variation of shell morphology as shown by the distinction of physiographic province groups, although intensive study of habitat variation was not performed in this study. Both GM and TM methods resulted in significant differences among physiographic provinces. These findings further suggest an environmental influence on overall external shell

morphology, agreeing with previous studies (Goodfriend 1986; Fiorentino et al. 2008; Vergara et al. 2017). The smaller MOTU dataset, comparatively, exhibited large morphological overlap between MOTU groups. However, results were significant for distinction from the TM groupings (see **Table 4**). This significance is most likely the result of population-based similarity in shell size, rather than the respective MOTU, of which many consist of multiple populations. Further, the GM groups did not exhibit significance with the MOTU dataset. The small sample size is a potential drawback to the utilization of these morphometric approaches. Terrestrial micromolluscs are notoriously difficult to sample (Boag 1982; Durkan et al. 2013), and sampling in cave environments significantly increases this difficulty. Moreover, as many of these populations remain understudied, morphometric methods may negatively impact populations subject to high amounts of collection and disturbance. This said, utilization of molecular barcodes may be most useful in the identification of these terrestrial micromolluscs (Weigand et al. 2011, 2014).

Taxonomic and Conservation Implications

The discovery of cryptic evolutionary lineages within *H. barri* has significant conservation implications. Recent reassessment of the conservation status of *H. barri* listed this species as Vulnerable (G3) under NatureServe criteria and Least Concern (LC) under the IUCN Red List criteria (Gladstone et al. 2018). Though our study suggests that this species is more geographically wide-spread than previously known, the distribution of individual MOTUs is greatly reduced, sometimes being restricted to a single cave. However, this species' presence in both karst regions despite separation by a considerable amount of non-karst strata and the discovery of a single specimen from surface habitat (see **Table 1**) suggests that it may not be

limited to cave systems. Rather, like other *Helicodiscus* species, *H. barri* could be highly calciphilic, dwelling in rock talus piles or potentially interstitial habitats (Gladstone et al. 2018; Dr. Jeff Nekola, personal comm.). Few studies have investigated the significance of epikarst and other subsurface habitats to troglobitic fauna in North America (Culver et al. 2012), and a more intensive sampling effort may be necessary to assess the importance of these habitats in facilitating the dispersal of such snail fauna.

This study offers an important first step in outlining the presence of cryptic lineages within *H. barri*. However, many aspects of this species' ecology and life history remain unknown, and the subsequent assessment of distinguishing ecology or habitat requirements for these cryptic groups is essential for their conservation and management. As with other recently discovered cryptic species, additional study of MOTU distribution, ecology, and conservation status are all necessary (Niemiller et al. 2013; Schlesinger et al. 2018).

REFERENCES

- Adams, D.C., and E. Otarola-Castillo. 2013. *geomorph*: an R package for the collection and analysis of geometric morphometric shape data. *Methods in Ecology and Evolution* 4: 393–399.
- Adams, D. C., E. Otarola-Castillo and E. Sherratt. 2014 *geomorph*: Software for geometric morphometric analyses. R package version 2.0. <http://cran.r-project.org/web/packages/geomorph/index.html>.
- Anthony, D. M., and D. E. Granger. 2004. A Late Tertiary Origin for Multilevel Caves Along the Western Escarpment of the Cumberland Plateau, Tennessee and Kentucky, Established by Cosmogenic super (26) Al and super (10) Be. *Journal of Cave and Karst Studies* 66(2): 46–55.
- Armbruster, J. W., M. L. Niemiller, and P. B. Hart. 2016. Morphological Evolution of the Cave-, Spring-, and Swampfishes of the Amblyopsidae (Percopsiformes). *Copeia* 104(3): 763–777.
- Avise, J. C. 2000. *Phylogeography: the history and formation of species*. Harvard University Press, Cambridge, MA.
- Barker, G. M. 2001. Gastropods on land: phylogeny, diversity, and adaptive morphology. In G.M. Barker (editor) *The Biology of Terrestrial Molluscs*, pp. 1–146. CABI Publishing, Wallingford, New Zealand.
- Barr, T. C. 1961. *Caves of Tennessee*. Bulletin 64. Tennessee Division of Geology, Nashville, TN.
- Barr, T. C. 1968. Cave ecology and the evolution of troglobites. In T. Dobzhansky, M. K. Hecht, and W. C. Steere (editors) *Evolutionary Biology*, pp. 35–102. Springer, Boston, MA.

- Barr, T. C. 1969. Evolution of the (Coleoptera) Carabidae in the Southern Appalachians. In P. C. Holt, M. K. Roane, B. C. Parker (editors) *The Distributional History of the Biota of the Southern Appalachians*, pp. 67–92. University of Virginia Press, Charlottesville, VA.
- Bickford, D., D. J. Lohman, N. S. Sodhi, P. K. L. Ng, R. Meier, K. Winker, K. K. Ingram, and I. Das. 2007. Cryptic species as a window on diversity and conservation. *Trends in Ecology & Evolution* 22(3): 148–155.
- Boag, D. A. 1982. Overcoming sampling bias in studies of terrestrial gastropods. *Canadian Journal of Zoology* 60: 1289–1292.
- Boc, A., A. B. Diallo, and V. Makarenkov. 2012. T-REX: a web server for inferring, validating and visualizing phylogenetic trees and networks. *Nucleic Acids Research* 40(1): 573–579.
- Bookstein, F. L. 1997. *Morphometric tools for landmark data: geometry and biology*. Cambridge University Press, Cambridge, UK.
- Bryson, R. W., L. Prendini, W. E. Savary, and P. B. Pearman. 2014. Caves as microrefugia: Pleistocene phylogeography of the troglomorphic North American scorpion *Pseudouroctonus reddelli*. *BMC Evolutionary Biology* 14(1): 9.
- Buhay, J. E., G. Moni, N. Mann, and K. A. Crandall. 2007. Molecular taxonomy in the dark: evolutionary history, phylogeography, and diversity of cave crayfish in the subgenus *Aviticambarus*, genus *Cambarus*. *Molecular Phylogenetics and Evolution* 42(2): 435–448.
- Buhay, J. E. and K. A. Crandall. 2009. Taxonomic revision of cave crayfish in the genus *Cambarus* subgenus *Aviticambarus* (Decapoda: Cambaridae) with descriptions of two new species, *C. speleocoopi* and *C. laconensis*, endemic to Alabama, USA. *Journal of Crustacean Biology* 29: 121–134.

- Burch, J. B. 1962. *How to Know the Eastern Land Snails*. In C. William (editor) Brown Company Publishers, Dubuque, IA. 214 pp.
- Burress, P. B. H., E. D. Burress, and J. W. Armbruster. 2017. Body shape variation within the Southern Cavefish, *Typhlichthys subterraneus* (Percopsiformes: Amblyopsidae). *Zoomorphology*: 1–13.
- Cameron, R. A. D., and B. M. Pokryszko. 2005. Estimating the species richness and composition of land mollusc communities: Problems, consequences and practical advice. *Journal of Conchology* 38(5): 529–548.
- Carstens, B. C., T. A. Pelletier, N. M. Reid, and J. D. Satler. 2013. How to fail at species delimitation. *Molecular Ecology* 22(17): 4369–4383.
- Chiba, S. 1996. A 40,000-year record of discontinuous evolution of island snails. *Paleobiology* 22(2): 177–188.
- Chiba, S. 1999. Accelerated evolution of land snails *Mandarina* in the oceanic Bonin islands: evidence from mitochondrial DNA sequences. *Evolution* 53: 460–471.
- Christman, M. C., and D. C. Culver. 2001. The relationship between cave biodiversity and available habitat. *Journal of Biogeography* 28(3): 367–380.
- Christman, M. C., D. C. Culver, M. K. Madden, and D. White. 2005. Patterns of endemism of the eastern North American cave fauna. *Journal of Biogeography* 32(8): 1441–1452.
- Clements, R., N. S. Sodhi, M. Schilthuizen, and P. K. L. Ng. 2006. Limestone karsts of Southeast Asia: imperiled arks of biodiversity. *AIBS Bulletin* 56(9): 733–742.

- Clements, R., P. K. L. Ng, X. Lu, S. Ambu, M. Schilthuizen, and C.J.A. Bradshaw. 2008. Using biogeographical patterns of endemic land snails to improve conservation planning for limestone karsts. *Biological Conservation* 141(11): 2751–2764.
- Colgan, D. J., W. F. Ponder, and P. E. Eggler. 2000. Gastropod evolutionary rates and phylogenetic relationships assessed using partial 28S rDNA and histone H3 sequences. *Zoologica Scripta* 29(1): 29–63.
- Coney, C. C., W. A. Tarpley, and R. Bohannon. 1982. Ecological studies of land snails in the Hiawassee River Basin of Tennessee, U.S.A. *Malacological Review* 15: 69–106.
- Cooper, S. J. B., S. Hinze, R. Leys, C. H. S. Watts, and W. F. Humphreys. 2002. Islands under the desert: molecular systematics and evolutionary origins of stygobitic water beetles (Coleoptera: Dytiscidae) from central Western Australia. *Invertebrate Systematics* 16(4): 589–590.
- Culver, D. C. 1970. Analysis of simple cave communities I. Caves as islands. *Evolution* 24(2): 463–474.
- Culver, D. C., and T. Pipan. 2009. *The Biology of Caves and Other Subterranean Habitats*. 2nd. Oxford, United Kingdom: Oxford University Press.
- Culver, D. C., M. C. Christman, W. R. Elliott, H. H. Hobbs, and J. R. Reddell. 2003. The North American obligate cave fauna: regional patterns. *Biodiversity & Conservation* 12(3): 441–468.
- Culver, D. C., T. Pipan, and K. Schneider. 2009. Vicariance, dispersal and scale in the aquatic subterranean fauna of karst regions. *Freshwater Biology* 54(4): 918–929.

- Culver, D. C., A. Brancelj, and T. Pipan. 2012. Epikarst communities. In W. B. White and D. C. Culver (editors) *Encyclopedia of Caves (Second Edition)*, pp. 288–295. Elsevier, Oxford, U.K.
- Dalquist, W. W., and F. B. Stangl. 1984. Late Pleistocene and early Recent mammals from Fowlkes Cave, southern Culbertson County, Texas. *Carnegie Museum of Natural History Special Publication* 8: 432–455.
- Davies, W. E. 1953. Geology of Pennsylvania caves. *National Speleological Society Bulletin* 15: 3–9.
- Davison, A., R. L. E. Blackie, and G. P. Scothern. 2009. DNA barcoding of stylommatophoran land snails: a test of existing sequences. *Molecular Ecology Resources* 9: 1092–1101.
- Dayrat, B. 2005. Towards integrative taxonomy. *Biological Journal of the Linnean Society* 85(3): 407–415.
- Dinkins, B. J., and G. R. Dinkins. 2018. An Inventory of the Land Snails and Slugs (Gastropoda: Caenogastropoda and Pulmonata) of Knox County, Tennessee. *American Malacological Bulletin* 36(1): 1–22.
- Douglas, D. A., D. C. Dourson, and R. S. Caldwell. 2014. The Land Snails of White Oak Sinks, Great Smoky Mountain National Park, Tennessee. *Southeastern Naturalist* 13(1): 166–175.
- Dourson, D. C. 2007. A selected land snail compilation of the Central Knobstone escarpment on Furnace Mountain in Powell County Kentucky. *Journal of the Kentucky Academy of Science* 68: 119–131.
- Dourson, D. C. 2010. *Kentucky's Land Snails and Their Ecological Communities*. Goatslug Publications, Bakersville, NC.

- Duminil, J., and M. Di Michele. 2009. Plant species delimitation: a comparison of morphological and molecular markers. *Plant Biosystems* 143(3): 528–542.
- Durkan, T. H., N. W. Yeung, W. M. Meyer, K. A. Hayes, and R. H. Cowie. 2013. Evaluating the efficacy of land snail survey techniques in Hawaii: implications for conservation throughout the Pacific. *Biodiversity and Conservation* 22(13-14): 3223–3232.
- Emberton, K. C. 1995. When shells do not tell: 145 million years of evolution in North America's polygyrid land snails, with a revision and conservation priorities. *Malacologia* 37: 69–110.
- Eme, D., M. Zagmajster, T. Delić, C. Fišer, J. F. Flot, L. Konecny-Dupré, S. Pálsson, F. Stoch, V. Zakšek, C. J. Douady, and F. Malard. 2018. Do cryptic species matter in macroecology? Sequencing European groundwater crustaceans yields smaller ranges but does not challenge biodiversity determinants. *Ecography* 41(2): 424–436.
- Eshelman, R., and M. Hager. 1984. Two Irvingtonian (medial Pleistocene) vertebrate faunas from north-central Kansas. *Contributions in Quaternary Vertebrate Paleontology: a volume in memorial to John E. Guilday, Special Publication of Carnegie Museum of Natural History* 8: 384–404.
- Fenneman, N. M. 1917. Physiographic subdivision of the United States. *Proceedings of the National academy of Sciences of the United States of America* 3(1): 17–22.
- Finston, T. L., M. S. Johnson, W. F. Humphreys, S. M. Eberhard, and S. A. Halse. 2007. Cryptic speciation in two widespread subterranean amphipod genera reflects historical drainage patterns in an ancient landscape. *Molecular Evolution* 16: 355–365.

- Fiorentino, V., N. Salomone, G. Manganelli, and F. Giusti. 2008. Phylogeography and morphological variability in land snails: the Sicilian *Marmorana* (Pulmonata, Helicidae). *Biological Journal of the Linnean Society* 94: 809–823.
- Floyd, R., E. Abebe, A. Papert, and M. Blaxter. 2002. Molecular barcodes for soil nematode identification. *Molecular Ecology* 11(4): 839–850.
- Folmer, O., M. Black, W. Hoeh, R. Lutz, and R. Vrijenhoek. 1994. DNA primers for amplification of mitochondrial cytochrome c oxidase subunit I from diverse metazoan invertebrates. *Molecular Marine Biology and Biotechnology* 3: 294–299.
- Gladstone, N. S., E. T. Carter, M. L. McKinney, and M. L. Niemiller. 2018. Status and Distribution of the Cave-Obligate Land Snails in the Appalachians and Interior Low Plateau of the Eastern United States. *American Malacological Bulletin* 36(1): 62–78.
- Goodfriend, Glenn A. 1986. Variation in land-snail shell form and size and its causes: a review. *Systematic Biology* 35(2): 204–223.
- Guilday, J. E., P. W. Parmalee, and H. W. Hamilton. 1977. The Clark's Cave bone deposit and the Pleistocene paleoecology of the central Appalachian Mountains of Virginia. *Bulletin of Carnegie Museum of Natural History* 2: 1–87.
- Guiller, A., L. Madec, and J. Daguzan. 1994. Geographical patterns of genetic differentiation in the land snail *Helix aspersa* Müller (Gastropoda: Pulmonata). *Journal of Molluscan Studies* 60: 205–221.
- Harris, J. D., A. F. Ferreira, and A. M. De Frias Martins. 2013. High levels of mitochondrial DNA diversity within oxychilid land snails (subgenus *Drouetia* Gude, 1911) from São Miguel island, Azores. *Journal of Molluscan Studies* 79(2): 177–182.

- Hasegawa, M., H. Kishino, and T. Yano. 1985. Dating of the human-ape splitting by a molecular clock of mitochondrial DNA. *Journal of Molecular Evolution* 22(2): 160–174.
- Hermesen, E. J., and J. R. Hendricks. 2008. W(h)ither fossils? Studying morphological character evolution in the age of molecular sequences. *Annals of the Missouri Botanical Garden* 95(1): 72–100.
- Hewitt, G. M. 1996. Some genetic consequences of ice ages, and their role in divergence and speciation. *Biological journal of the Linnean Society* 58(3): 247–276.
- Hobbs, H. H. 2012. Diversity patterns in the United States. In W. B. White and D. C. Culver (editors) *Encyclopedia of Caves (Second Edition)*, pp. 251–264. Elsevier, Oxford, U.K.
- Holsinger, J. R. 1988. Troglobites: the evolution of cave-dwelling organisms. *American Scientist* 76(2): 146–153.
- Hotopp, K. P., T. Pearce, J. C. Nekola, J. Slapcinsky, and D. C. Dourson, M. Winslow, G. Kimber, and B. Watson. 2013. Land Snails and Slugs of the Mid-Atlantic and Northeastern United States. Carnegie Museum of Natural History, Pittsburgh, PA, USA.
- Hubricht, L. 1962. New species of *Helicodiscus* from the eastern United States. *The Nautilus* 75(3): 102–107.
- Hubricht, L. 1985. The distributions of the native land mollusks of the eastern United States. *Fieldiana n.S.* 24: 1–191.
- Huson, D. H., and D. Bryant. 2005. Application of phylogenetic networks in evolutionary studies. *Molecular Biology and Evolution* 23(2): 254–267.
- Jochum, A., R. Slapnik, A. Klussmann-Kolb, B. Pall-Gergely, M. Kampschulte, G. Martels, M. Vrabec, C. Nesselhauf, and A. M. Weigand. 2015. Groping through the black box of variability: An integrative taxonomic and nomenclatural re-evaluation of *Zospeum*

- isselianum* Pollonera, 1887 and allied species using new imaging technology (Nano-CT, SEM), conchological, historical and molecular data (Ellobioidea, Carychiidae). *Subterranean Biology* 16: 123–165.
- Juan, C., and B. C. Emerson. 2010. Evolution underground: shedding light on the diversification of subterranean insects. *Journal of Biology* 9(3): 17.
- Juan, C., M. T. Guzik, D. Jaume, and S. J. B. Cooper. 2010. Evolution in caves: Darwin's 'wrecks of ancient life' in the molecular era. *Molecular Ecology* 19: 3865–3880.
- Kano, Y., S. Chiba, and T. Kase. 2002. Major adaptive radiation in neritopsine gastropods estimated from 28S rRNA sequences and fossil records. *Proceedings of the Royal Society of London B: Biological Sciences* 269(1508): 2457–2465.
- Kapli, P., S. Lutteropp, J. Zhang, K. Kobert, P. Pavlidis, A. Stamatakis, and T. Flouri. 2017. Multi-rate Poisson tree processes for single-locus species delimitation under maximum likelihood and Markov chain Monte Carlo. *Bioinformatics* 33(11): 1630–1638.
- Kimura, M. 1980. A simple method for estimating evolutionary rates of base substitutions through comparative studies of nucleotide sequences. *Journal of Molecular Evolution* 16: 111–120.
- Kumar, S., G. Stecher, M. Li, C. Knyaz, and K. Tamura. 2018. MEGA X: Molecular Evolutionary Genetics Analysis across Computing Platforms. *Molecular Biology and Evolution* 35(6): 1547–1549.
- Lanfear, R., B. Calcott, S. Y. W. Ho, and S. Guindon. 2012. PartitionFinder: combined selection of partitioning schemes and substitution models for phylogenetic analyses. *Molecular Biology and Evolution* 29(6): 1695–1701.

- Leray, V. L., J. Caravas, M. Friedrich, and K. S. Zigler. 2019. Mitochondrial sequence data indicate “Vicariance by Erosion” as a mechanism of species diversification in North American Ptomaphagus (Coleoptera, Leiodidae, Cholevinae) cave beetles. *Subterranean Biology* 29: 35–57.
- Leys, R., C. H. S. Watts, S. J. B. Cooper, and W. F. Humphreys. 2003. Evolution of subterranean diving beetles (Coleoptera: Dytiscidae Hydroporini, Bidessini) in the arid zone of Australia. *Evolution* 57(12): 2819–2834.
- Librado, P., and J. Rozas. 2009. DnaSP v5: a software for comprehensive analysis of DNA polymorphism data. *Bioinformatics* 25(11): 1451–1452.
- Liew, T., R. Clements, and M. Schilthuizen. 2008. Sampling micromolluscs in tropical forests: one size does not fit all. *Zoosymposia* 1: 271–280.
- Liggert, G. A. 1997. The beckerdie local biota (early Hemphillian) and the first Tertiary occurrence of a crocodylian from Kansas. *Transactions of the Kansas Academy of Sciences* 100(3-4): 101–108.
- Liu, H., and R. Hershler. 2007. A test of the vicariance hypothesis of western North American freshwater biogeography. *Journal of Biogeography* 34(3): 534–548.
- Loria, S. E., K. S. Zigler, and J. L. Lewis. 2011. Molecular phylogeography of the troglolithic millipede *Tetracion* Hoffman, 1956 (Diplopoda, Callipodida, Abacionidae). *International Journal of Myriapodology* 5: 35–48.
- Losos, J. B., and L. D. Mahler. 2010. Adaptive radiation: the interaction of ecological opportunity, adaptation, and speciation. In: M. A. Bell et al. (editors), *Evolution since Darwin: the first 150 years*, pp. 381–420. Sinauer Associates. Sunderland, MA.

- Lydeard, C., R. H. Cowie, W. F. Ponder, A. E. Bogan, P. Bouchet, S. A. Clark, K. F. Cummings, T. J. Frest, O. Gargominy, D. G. Herbert, R. Hershler, K. E. Perez, B. Roth, M. Seddon, E. E. Strong, and F. G. Thompson. 2004. The global decline of nonmarine mollusks. *BioScience* 54: 321–330.
- McGuire, J. A., C. W. Linkem, M. S. Koo, D. W. Hutchison, K. A. Lappin, D. I. Orange, J. Lemos-Espinal, B. R. Riddle, and J. R. Jaeger. 2007. Mitochondrial introgression and incomplete lineage sorting through space and time: phylogenetics of crotaphytid lizards. *Evolution: International Journal of Organic Evolution* 61(12): 2879–2897.
- Miller, J. P. 2016. Geometric morphometric analysis of the shell of *Cerion mumia* (Pulmonata: Cerionidae) and related species. *Folia Malacologica* 24(4): 239–250.
- Moneymaker, B. C. 1948. Some broad aspects of limestone solution in the Tennessee Valley. *Transactions of the American Geophysical Union* 29(1): 93–96.
- Moulds, T. A., N. Murphy, M. Adams, T. Reardon, M. S. Harvey, J. Jennings, and A. D. Austin. 2007. Phylogeography of cave pseudoscorpions in southern Australia. *Journal of Biogeography* 34: 951–962.
- Murphy, N. P., M. F. Breed, M. T. Guzik, S. J. B. Cooper, and A. D. Austin. 2012. Trapped in desert springs: phylogeography of Australian desert spring snails. *Journal of Biogeography* 39(9): 1573–1582.
- Myers, N., R. A. Mittermeier, C. G. Mittermeier, G. A. B. Da Fonseca, and J. Kent. 2000. Biodiversity hotspots for conservation priorities. *Nature* 403(6772): 853–858.
- Nekola, J. C. 2005. Geographic variation in richness and shell size of eastern North American land snail communities. *Records of the Western Australian Museum Supplement* 68: 39–51.

- Nekola, J. C. 2014. Overview of the North American terrestrial gastropod fauna. *American Malacological Bulletin* 32(2): 225–235.
- Nekola, J. C., and B. F. Coles. 2010. Pupillid land snails of eastern North America. *American Malacological Bulletin*. 28: 29–57.
- Niemiller, M. L., B. M. Fitzpatrick, and B. T. Miller. 2008. Recent divergence with gene flow in Tennessee cave salamanders (Plethodontidae: Gyrinophilus) inferred from gene genealogies. *Molecular Ecology* 17(9): 2258–2275.
- Niemiller, M. L., T. J. Near, and B. M. Fitzpatrick. 2011. Delimiting species using multilocus data: diagnosing cryptic diversity in the southern cavefish, *Typhlichthys subterraneus* (Teleostei: Amblyopsidae). *Evolution* 66(3): 846–866.
- Niemiller, M. L., and K. S. Zigler. 2013. Patterns of cave biodiversity and endemism in the Appalachians and Interior Plateau of Tennessee, USA. *PLoS One* 8(5): e64177.
- Niemiller, M. L., B. M. Fitzpatrick, P. Shah, L. Schmitz, and T. J. Near. 2013. Evidence for repeated loss of selective constraint in rhodopsin of amblyopsid cavefishes (Teleostei: Amblyopsidae). *Evolution* 67: 732–748.
- Niemiller, M. L., M. L. Porter, J. Keany, H. Gilbert, D. W. Fong, D. C. Culver, C. S. Hobson, K. D. Kendall, M. A. Davis, and S. J. Taylor. 2018. Evaluation of eDNA for groundwater invertebrate detection and monitoring: a case study with endangered *Stygobromus* (Amphipoda: Crangonyctidae). *Conservation Genetics Resources* 10(2): 247–257.
- Palumbi, S., A. Martin, S. Romano, W. O. McMillan, L. Stice, and G. Grabowski. 1991. The Simple Fool's Guide to PCR. Version 2.0. University of Hawaii, Honolulu.

- Pearce, T. A., and A. Örstan. 2006. Terrestrial Gastropoda. In C. F. Sturm, T. A. Pearce and A. Valdés (editors) *The Mollusks: A Guide to Their Study, Collection, and Preservation*. American Malacological Society. U.S.A. pp. 261–285.
- Perez, K. E., N. Defreitas, J. Slapcinsky, R. L. Minton, F. E. Anderson, and T. A. Pearce. 2014. Molecular phylogeny, evolution of shell shape, and DNA barcoding in Polygyridae (Gastropoda: Pulmonata), an endemic North American clade of land snails. *American Malacological Bulletin* 32(1): 1–31.
- Perez, S. I., J. A. F. Diniz-Filho, V. Bernal, and P. N. Gonzalez. 2010. Spatial regression techniques for inter-population data: studying the relationships between morphological and environmental variation. *Journal of Evolutionary Biology* 23(2): 237–248.
- Pilsbry, H. A. 1948. Land Mollusca of North America (north of Mexico). Volume II, Part II. The Academy of Natural Sciences of Philadelphia. Philadelphia, PA.
- Pons, J., T. G. Barraclough, J. Gomez-Zurita, A. Cardoso, D. P. Duran, S. Hazell, S. Kamoun, W. D. Sumlin, and A. P. Vogler. 2006. Sequence-based species delimitation for the DNA taxonomy of undescribed insects. *Systematic Biology* 55(4): 595–609.
- Porter, M. L. 2007. Subterranean biogeography: what have we learned from molecular techniques. *Journal of Cave and Karst Studies* 69(1): 179–186.
- Puillandre, N., A. Lambert, S. Brouillet, and G. Achaz. 2012. ABGD, Automatic Barcode Gap Discovery for primary species delimitation. *Molecular Ecology* 21(8): 1864–1877.
- Oksanen J., G. F. Blanchet, M. Friendly, R. Kindt, P. Legendre, D. McGlinn, P. R. Minchin, R. B. O'Hara, G. L. Simpson, P. Solymos, M. H. H. Stevens, E. Szoecs, and H. Wagner. 2018 *vegan*: Community Ecology Package. R package version 2.5-1. <https://CRAN.R-project.org/package=vegan>

- R Core Team (2014). R: A language and environment for statistical computing. R Foundation for Statistical Computing, Vienna, Austria. URL <http://www.R-project.org/>.
- Rambaut, A., and A. J. Drummond. 2007. Tracer v. 1.4, available from <http://beast.bio.ed.ac.uk/Tracer>.
- Razkin, O., B. J. Gomez-Moliner, K. Vardinoyannis, A. Martinez-Orti, and M. J. Madeira. 2017. Species delimitation for cryptic species complexes: case study of *Pyramidula* (Gastropoda, Pulmonata). *Zoologica Scripta* 46: 55–72.
- Rinker, G. C. 1949. Tremarctotherium from the Pleistocene of Meade County, Kansas. *Contributions from the Museum of Paleontology, University of Michigan* 7(6): 107–112.
- Rohlf, F. J. 2015. The tps series of software. *Hystrix, the Italian Journal of Mammalogy* 26: 1–4.
- Ronquist, F., M. Teslenko, P. Van Der Mark, D. L. Ayres, A. Darling, S. Höhna, B. Larget, L. Liu, M. A. Suchard, and J. P. Huelsenbeck. 2012. MrBayes 3.2: efficient Bayesian phylogenetic inference and model choice across a large model space. *Systematic Biology* 61(3): 539–542.
- Rubinoff, D. 2006. Utility of mitochondrial DNA barcodes in species conservation. *Conservation Biology* 20(4): 1026–1033.
- Schlesinger, M. D., J. A. Feinberg, N. H. Nazdrowicz, J. D. Kleopfer, J. C. Beane, J. F. Bunnell, J. Burger, E. Corey, K. Gipe, J. W. Jaycox, and E. Kiviat. 2018. Follow-up ecological studies for cryptic species discoveries: Decrypting the leopard frogs of the eastern US. *PloS One* 13(11): e0205805.
- Schultz, G. E., and E. P. Cheatum. 1970. *Bison occidentalis* and associated invertebrates from the late Wisconsin of Randall County, Texas. *Journal of Paleontology* 44(5): 836–850.

- Slaughter, B. H. 1966. The Moore Pit local fauna; Pleistocene of Texas. *Journal of Paleontology* 40(1): 78–91.
- Smith, U. E., and J. R. Hendricks. 2013. Geometric morphometric character suites as phylogenetic data: extracting phylogenetic signal from gastropod shells. *Systematic Biology* 62(3): 366–385.
- Snowman, C. V., K. S. Zigler, and M. Hedin. 2010. Caves as islands: mitochondrial phylogeography of the cave-obligate spider species *Nesticus barri* (Araneae: Nesticidae). *Journal of Arachnology* 38: 49–56.
- Sokal, R. R. & Oden, N. L. 1978. Spatial autocorrelation in biology. 1. Methodology. *Biological Journal of the Linnean Society* 10: 199–228.
- Stamatakis, A. 2014. RAxML version 8: a tool for phylogenetic analysis and post-analysis of large phylogenies. *Bioinformatics* 30(9): 1312–1313.
- Stankowski, S. 2011. Extreme, continuous variation in an island snail: local diversification and association of shell form with the current environment. *Biological Journal of the Linnean Society* 104: 756–769.
- Thacker, R. W., and M. G. Hadfield. 2000. Mitochondrial phylogeny of extant Hawaiian tree snails (Achatinellinae). *Molecular Phylogenetics and Evolution* 16(2): 263–270.
- Thomaz, D., A. Guiller, and B. Clarke. 1996. Extreme divergence of mitochondrial DNA within species of pulmonated land snails. *Proceedings of the Royal Society of London Series B – Biological Sciences* 263: 363–368.
- Uit de Weerd, D., W. H. Piel, and E. Gittenberger. 2004. Widespread polyphyly among Aloiinae land snail genera: when phylogeny mirrors biogeography more closely than morphology. *Molecular Phylogenetics and Evolution* 33: 533–548.

- Van Riel, P., K. Jordaens, N. Van Houtte, A. M. F. Martins, R. Verhagen, and T. Backeljau. 2005. Molecular systematics of the endemic Leptaxini (Gastropoda: Pulmonata) on the Azores islands. *Molecular Phylogenetics and Evolution* 37: 132–143.
- Vergara, D., J. A. Fuentes, K. S. Stoy, and C. M. Lively. 2017. Evaluating shell variation across different populations of a freshwater snail. *Molluscan Research* 37(2): 120–132.
- Wagner, P. J. 2001. Gastropod phylogenetics: progress, problems, and implications. *Journal of Paleontology* 75: 1128–1140.
- Weary, D. J., and D. H. Doctor. 2014. Karst in the United States: A digital map compilation and database. USGS Open File Report 2014–1156; Available: <http://pubs.usgs.gov/of/2014/1156/>
- Webb III, T., and P. J. Bartlein. 1992. Global changes during the last 3 million years: climatic controls and biotic responses. *Annual review of Ecology and Systematics* 23(1): 141–173.
- Weckstein, J. D., K. P. Johnson, J. D. Murdoch, J. K. Krejca, D. M. Tayika, G. Veni, J. R. Reddell, and S. J. Taylor. 2016. Comparative phylogeography of two codistributed subgenera of cave crickets (Orthoptera: Rhaphidophoridae: *Ceuthophilus* spp.). *Journal of Biogeography* 43: 1450–1463.
- Weigand, A. M., A. Jochum, M. Pfenninger, D. Steinke, and A. Klussmann-Kolb. 2011. A new approach to an old conundrum—DNA barcoding sheds new light on phenotypic plasticity and morphological stasis in microsnails (Gastropoda, Pulmonata, Carychiidae). *Molecular Ecology Resources* 11(2): 255–265.
- Weigand, A. M., Götze, M. C. and Jochum, A. 2012. Outdated but established?! Conchologically driven species delineations in microgastropods (Carychiidae, Carychium). *Organisms Diversity & Evolution* 12(4): 377–386.

- Weigand, A. M., A. Jochum, and A. Klussmann-Kolb. 2014. DNA barcoding cleans house through the Carychiidae (Eupulmonata, Ellobioidea). *American Malacological Bulletin* 32(2): 236–245.
- Wetmore, A. 1962. Notes on fossil and subfossil birds. *Smithsonian Miscellaneous Collections* 145(2): 1–17.
- White, W. B. 2009. The evolution of Appalachian fluviokarst: competition between stream erosion, cave development, surface denudation, and tectonic uplift. *Journal of Cave and Karst Studies* 71(3): 159–167.
- Zhang, J., P. Kapli, P. Pavlidis, and A. Stamatakis. 2013. A general species delimitation method with applications to phylogenetic placements. *Bioinformatics* 29(22): 2869–2876.
- Zharkikh, A. 1994. Estimation of evolutionary distances between nucleotide sequences. *Journal of Molecular Evolution* 39(3): 315–329.

APPENDIX

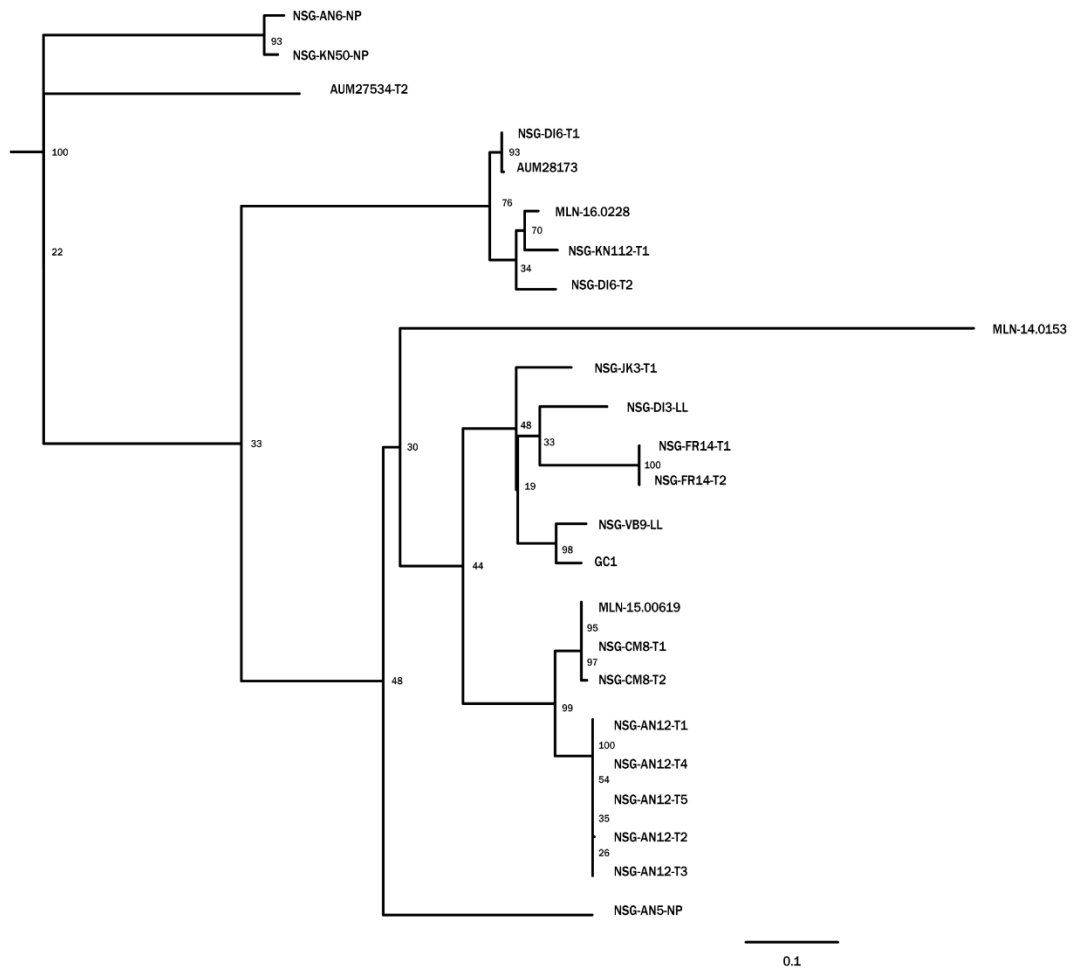


Figure A1. CO1 (704 bp) phylogram of *H. barri* generated from RAxML. Outgroup not shown due to long branch length.

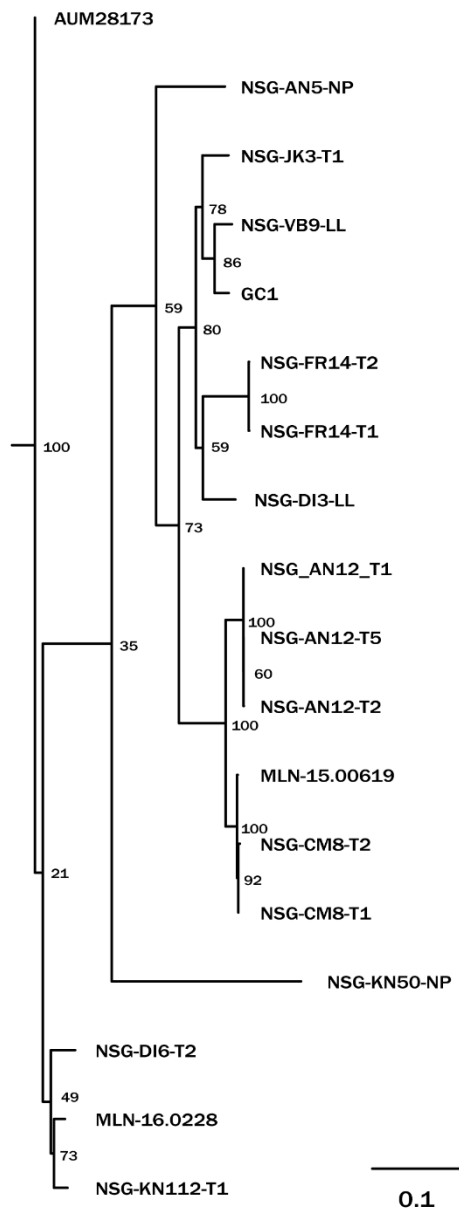


Figure A2. *mtDNA + nDNA* (CO1 + 16S + 28S + H3; 3040 bp) phylogram generated of *H. barri* from RAxML. Outgroup not shown due to long branch length.

Table A1. GenBank accession numbers for all sequence data.

ID	16S	28S	CO1	H3
AUM-27534-T2	MK541096.1	MK590382.1	MK674986.1	
AUM-27855	MK541097.1	MK590383.1		MK675010.1
AUM-28173	MK541098.1	MK590384.1	MK674987.1	MK675011.1
AUM-28348	MK541099.1	MK590385.1		MK675012.1
GC1	MK541100.1	MK590386.1	MK674988.1	MK675013.1
MLN-13-000				
MLN-13-056	MK541101.1	MK590387.1		MK675014.1
MLN-14-007		MK590388.1		MK675015.1
MLN-14-015.3		MK590389.1	MK674989.1	
MLN-14-054.12	MK541102.1	MK590390.1		
MLN-15-006.19	MK541103.1	MK590391.1	MK674990.1	MK675016.1
MLN-16-022.8	MK541104.1	MK590392.1	MK674991.1	MK675017.1
NSG-AN12-T1	MK541105.1	MK590393.1	MK674992.1	MK675018.1
NSG-AN12-T2	MK541106.1	MK590394.1	MK674993.1	MK675019.1
NSG-AN12-T3		MK590395.1	MK674994.1	MK675020.1
NSG-AN12-T4	MK541107.1		MK674995.1	MK675021.1
NSG-AN12-T5	MK541108.1	MK590396.1	MK674996.1	MK675022.1
NSG-AN5-NP	MK541109.1	MK590397.1	MK674997.1	MK675023.1
NSG-AN6-NP	MK541110.1	MK590398.1	MK674998.1	
NSG-CM8-T1	MK541112.1	MK590399.1	MK674999.1	MK675024.1
NSG-CM8-T2	MK541113.1	MK590400.1	MK675000.1	MK675025.1
NSG-DI3-LL	MK541114.1	MK590401.1	MK675001.1	MK675026.1
NSG-DI6-T1	MK541115.1	MK590402.1	MK675002.1	
NSG-DI6-T2	MK541116.1	MK590403.1	MK675003.1	MK675027.1
NSG-FR14-T1	MK541117.1	MK590404.1	MK675004.1	MK675028.1
NSG-FR14-T2	MK541118.1	MK590405.1	MK675005.1	MK675029.1
NSG-JK3-T1	MK541121.1	MK590406.1	MK675006.1	MK675030.1
NSG-KN108-NP	MK541122.1			MK675031.1
NSG-KN112-T1	MK541123.1	MK590407.1	MK675007.1	MK675032.1
NSG-KN50-NP	MK541124.1	MK590408.1	MK675008.1	MK675033.1
NSG-RN5-LLB	MK541125.1	MK590409.1		
NSG-VB9-LL	MK541126.1	MK590410.1	MK675009.1	MK675034.1

Table A2. *H. barri* CO1 sequence distance matrix generated for 16 cave populations (labeled by the respective Cave Survey number). Values in italics represent within group variation when this data is available.

CO1	DK11	AMD6	OV440	FR9	CM8	AN22	AN12	AN5	AN6	DI3	DI6	FR14	JK3	KN112	KN50	VB9
DK11	-															
AMD6	0.189	-														
OV440	0.203	0.170	-													
FR9	0.196	0.232	0.194	-												
CM8	0.197	0.148	0.106	0.195	<i>0.004</i>											
AN22	0.194	0.043	0.153	0.218	0.160	-										
AN12	0.203	0.167	0.112	0.199	0.048	0.170	<i>0.000</i>									
AN5	0.211	0.179	0.144	0.211	0.156	0.179	0.160	-								
AN6	0.158	0.189	0.211	0.218	0.209	0.191	0.213	0.201	-							
DI3	0.206	0.158	0.086	0.201	0.117	0.148	0.115	0.153	0.201	-						
DI6	0.195	0.029	0.167	0.230	0.156	0.038	0.169	0.182	0.190	0.156	<i>0.055</i>					
FR14	0.187	0.172	0.096	0.203	0.118	0.167	0.122	0.146	0.208	0.089	0.177	<i>0.000</i>				
JK3	0.211	0.163	0.084	0.201	0.101	0.167	0.110	0.144	0.208	0.091	0.164	0.100	-			
KN112	0.194	0.053	0.167	0.220	0.156	0.029	0.170	0.184	0.194	0.151	0.053	0.170	0.167	-		
KN50	0.163	0.187	0.206	0.230	0.207	0.196	0.211	0.191	0.026	0.184	0.187	0.199	0.194	0.199	-	
VB9	0.199	0.167	0.036	0.184	0.104	0.158	0.112	0.144	0.222	0.086	0.170	0.096	0.081	0.167	0.206	-

Table A3. *H. barri* 16S sequence distance matrix generated for 20 cave populations (labeled by the respective Cave Survey number). Values in italics represent within group variation when this data is available.

16S	DK11	SM10	AMD6	DA4	OV440	MY11	JK3	CM8	AN22	AN12	AN5	AN6	DI3	DI6	FR14	KN108	KN112	KN50	RN5	VB9
DK11	-																			
SM10	0.177	-																		
AMD6	0.211	0.100	-																	
DA4	0.201	0.043	0.110	-																
OV440	0.182	0.014	0.100	0.038	-															
MY11	0.182	0.033	0.096	0.048	0.029	-														
JK3	0.189	0.022	0.103	0.036	0.017	0.026	<i>0.014</i>													
CM8	0.182	0.067	0.110	0.077	0.072	0.062	0.074	<i>0.000</i>												
AN22	0.211	0.100	0.019	0.115	0.100	0.086	0.103	0.110	-											
AN12	0.187	0.072	0.110	0.077	0.077	0.072	0.084	0.019	0.110	<i>0.000</i>										
AN5	0.187	0.067	0.105	0.081	0.062	0.067	0.069	0.091	0.105	0.096	-									
AN6	0.167	0.163	0.191	0.148	0.163	0.163	0.170	0.163	0.191	0.158	0.167	-								
DI3	0.187	0.033	0.100	0.043	0.029	0.029	0.026	0.077	0.100	0.081	0.072	0.158	-							
DI6	0.222	0.105	0.012	0.110	0.105	0.100	0.108	0.110	0.031	0.110	0.110	0.196	0.105	<i>0.024</i>						
FR14	0.187	0.043	0.091	0.048	0.038	0.038	0.036	0.077	0.091	0.077	0.067	0.163	0.033	0.098	<i>0.000</i>					
KN108	0.191	0.029	0.100	0.033	0.024	0.024	0.022	0.072	0.096	0.081	0.067	0.163	0.024	0.105	0.033	-				
KN112	0.215	0.105	0.005	0.115	0.105	0.100	0.108	0.115	0.024	0.115	0.110	0.196	0.105	0.017	0.096	0.105	-			
KN50	0.163	0.153	0.187	0.139	0.153	0.153	0.160	0.153	0.187	0.148	0.148	0.024	0.148	0.189	0.158	0.153	0.191	-		
RN5	0.182	0.014	0.100	0.038	0.000	0.029	0.017	0.072	0.100	0.077	0.062	0.163	0.029	0.105	0.038	0.024	0.105	0.153	-	
VB9	0.182	0.019	0.100	0.043	0.014	0.029	0.022	0.072	0.100	0.077	0.057	0.158	0.033	0.105	0.043	0.029	0.105	0.158	0.014	-

Table A4. *H. barri* 28S sequence distance matrix generated for 21 cave populations (labeled by the respective Cave Survey number). Values in italics represent within group variation when this data is available.

28S	DK1 1	SM1 0	AMD 6	DA4	OV44 0	MY1 1	DK7 2	FR9	JK3	CM8	AN2 2	AN1 2	AN5	AN6	DI3	DI6	FR1 4	KN11 2	KN5 0	RN5	VB 9	
DK11	-																					
SM10	0.012	-																				
AMD 6	0.010	0.002	-																			
DA4	0.010	0.002	0.000	-																		
OV44 0	0.010	0.002	0.000	0.00	-																	
MY11	0.010	0.002	0.000	0.00	0.000	-																
DK72	0.010	0.002	0.000	0.00	0.000	0.000	-															
FR9	0.012	0.016	0.016	0.01	0.016	0.016	0.016	-														
JK3	0.010	0.002	0.000	0.00	0.000	0.000	0.000	0.01	<i>0.00</i>													
CM8	0.010	0.002	0.000	0.00	0.000	0.000	0.000	0.01	0.00	<i>0.00</i>												
AN22	0.010	0.002	0.000	0.00	0.000	0.000	0.000	0.01	0.00	0.00	-											
AN12	0.011	0.002	0.000	0.00	0.000	0.000	0.000	0.01	0.00	0.00	0.000	<i>0.001</i>										
AN5	0.010	0.002	0.000	0.01	0.000	0.000	0.000	0.01	0.01	0.01	0.000	0.000	-									
AN6	0.000	0.012	0.010	0.00	0.010	0.010	0.010	0.01	0.00	0.00	0.010	0.011	0.01	-								
DI3	0.010	0.002	0.000	0.00	0.000	0.000	0.000	0.01	0.00	0.00	0.000	0.000	0.00	0.01	-							
DI6	0.011	0.003	0.001	0.00	0.001	0.001	0.001	0.01	0.00	0.00	0.001	0.001	0.00	0.01	0.00	<i>0.00</i>						
FR14	0.010	0.002	0.000	0.00	0.000	0.000	0.000	0.01	0.00	0.00	0.000	0.000	0.00	0.01	0.00	0.00	<i>0.00</i>					
KN11 2	0.010	0.002	0.000	0.01	0.000	0.000	0.000	0.01	0.01	0.01	0.000	0.000	0.01	0.00	0.01	0.01	0.01	0.01	0.01			
KN50	0.000	0.012	0.010	0.00	0.010	0.010	0.010	0.01	0.00	0.00	0.010	0.011	0.00	0.01	0.00	0.00	0.00	0.00	0.00	0.010	-	
RN5	0.010	0.002	0.000	0.00	0.000	0.000	0.000	0.01	0.00	0.00	0.000	0.000	0.00	0.01	0.00	0.00	0.00	0.00	0.00	0.000	0.010	-
VB9	0.010	0.002	0.000	0.00	0.000	0.000	0.000	0.01	0.00	0.00	0.000	0.000	0.00	0.01	0.00	0.00	0.00	0.00	0.00	0.000	0.010	0.00

Table A5. *H. barri* H3 sequence distance matrix generated for 18 cave populations (labeled by the respective Cave Survey number). Values in italics represent within group variation when this data is available.

H3	SM10	AMD6	DA4	OV440	MY11	DK72	CM8	AN22	AN12	AN5	DI3	DI6	FR14	JK3	KN108	KN112	KN50	VB9
SM10	-																	
AMD6	0.000	-																
DA4	0.004	0.004	-															
OV440	0.000	0.000	0.004	-														
MY11	0.000	0.000	0.004	0.000	-													
DK72	0.000	0.000	0.004	0.000	0.000	-												
CM8	0.000	0.000	0.004	0.000	0.000	0.000	<i>0.000</i>											
AN22	0.000	0.000	0.004	0.000	0.000	0.000	0.000	-										
AN12	0.000	0.000	0.004	0.000	0.000	0.000	0.000	0.000	<i>0.000</i>									
AN5	0.012	0.012	0.017	0.012	0.012	0.012	0.012	0.012	0.012	-								
DI3	0.000	0.000	0.004	0.000	0.000	0.000	0.000	0.000	0.000	0.012	-							
DI6	0.004	0.004	0.008	0.004	0.004	0.004	0.004	0.004	0.004	0.017	0.004	-						
FR14	0.002	0.002	0.006	0.002	0.002	0.002	0.002	0.002	0.002	0.014	0.002	0.006	<i>0.004</i>					
JK3	0.004	0.004	0.008	0.004	0.004	0.004	0.004	0.004	0.004	0.017	0.004	0.008	0.006	-				
KN108	0.000	0.000	0.004	0.000	0.000	0.000	0.000	0.000	0.000	0.012	0.000	0.004	0.002	0.004	-			
KN112	0.000	0.000	0.004	0.000	0.000	0.000	0.000	0.000	0.000	0.012	0.000	0.004	0.002	0.004	0.000	-		
KN50	0.012	0.012	0.017	0.012	0.012	0.012	0.012	0.012	0.012	0.000	0.012	0.017	0.014	0.017	0.012	0.012	-	
VB9	0.000	0.000	0.004	0.000	0.000	0.000	0.000	0.000	0.000	0.012	0.000	0.004	0.002	0.004	0.000	0.000	0.012	-

VITA

Nicholas Gladstone graduated from Hardin Valley Academy in December 2013, and proceeded to enroll at the University of Tennessee Knoxville in January 2014. He was originally pursuing a BS degree in Ecology and Evolutionary Biology, but decided to transition to the BS in Geology and Environmental Studies after becoming acquainted with Dr. Michael McKinney.

Dr. McKinney introduced Nicholas to scientific research, and advised him throughout his undergraduate career. During his undergraduate program, he began numerous research assistantships which eventually led him to his fascination in subterranean ecosystems. Nicholas now spends much of his time caving with his colleagues Dr. Matthew Niemiller and Dr. Evin Carter, looking at the unique animals that live underground.

Immediately following the completion of his BS, Nicholas was accepted into the Master of Geology program at the University of Tennessee Knoxville, beginning his graduate career in 2017. His research continues to focus on the evolution of cave animals and their conservation.